Aalto University
School of Electrical
Engineering

Ambient and quantum back-scatter communications

Prof. Riku Jäntti
Department of Communications and Networking

Aalto University
School of Electrical
Engineering

Part I: Ambient back-scatter communications

Ambient Backscatter Communications (AmBC)

Content

1. **Motivation**
2. **Basic principle**
3. **State-of-the art**
4. **Modulation methods**
5. **Propagation**
6. **Mitigating the direct path interference at the receiver**
7. **Co-existence with incumbent**
8. **Fundamental limits**
9. **Conclusions**

Aalto University
School of Electrical
Engineering

1. Motivation

Motivation

- The state-of-art IoT connectivity solutions can be two power hungry for ultra-low power / passive sensor devices.
- Transceiver is typically the most power hungry part of the IoT device.
- Can we communicate without having a transceiver in the IoT device?

Power can be harvested from Ambient RF Sources…

TABLE III
HOW MUCH POWER (EXPERIMENTAL RESULTS) CAN BE HARVESTED FROM AMBIENT RF SOURCES?

Power or Cycle time	RF Source	Dist. to Emitter	Frequency Band	Antenna Gain	Power Source strength	Harvester sensitivity	Literature
60 μW	TV	4.1 km	674-680 MHz	5 dBi Yagi-Uda	0.96 MW	N/A	Sample *et al.* [7], [16]
3s-CT	TV	10.4 km	539 MHz	6 dBi	1MW	-18 dBm	Parks *et al.* [6]
62.5μW	TV	4.2 km	539 MHz	6 dBi (wideband log-periodic)	1 MW	-10 dBm	Parks *et al.* [8]
126 μW (9 channels)	DTV	6.3 km	512-566 MHz	7 dBi	48 kW	-18.86 dBm	Vyas *et al.* [79]
927 μV (one rectenna)	FM	N/A†	81.9-84.7 MHz	1.83 dBi loop antenna	N/A	-20 dBm	Noguchi *et al.* [105]
2.39 μW	AM	50 m	1.278 MHz	rectenna	N/A	N/A	Otsuka *et al.* [106]
0.6 μW	AM	2.5 km	1.27 MHz	ferrite loop antenna	50 kW	-39 dBm	Wang *et al.* [107]
62 μW	AM	2.5 km	1 MHz	antenna-free LC circuit	10 kW	N/A	Leon-Gil *et al.* [108]
30.8 μW	WiFi	0.3 m	1.9-2.4 GHz	PCB antenna	24 dBm	N/A	Ishizaki *et al.* [31]
2.5μW	WiFi	0.115 m (0.92 m)	2.4 GHz	N/A (3 dBi)	2 dBm (20 dBm)	-16.5 dBm	Talla *et al.* [19]
>100s-CT	Cellular	>200 m	738 MHz	6 dBi	N/A	-18 dBm	Parks *et al.* [6]
600μV (140μV)	Cellular	received power density: 500 (60) $\mu W/m^2$	900, 1800, 2100 MHz	7 dBi dual-port triple-band L-probe microstrip patch rectenna	N/A	-30 dBm	Shen *et al.* [9]

- $\mu W/m^2$ denotes the power density at the harvester.
- CT: Cycle time.

† the distance and the power source strength are not available, but the received power at the harvesting point is -20 dBm.

…but it is quite low for powering active transceivers

TABLE I
COMPARISON OF COMMUNICATION TECHNOLOGIES.

Technology	Tag platform	Sensitivity (dBm)	Data Rate	Communication Range † (m)	Power Consumption (≈)	Power Source strength (dBm)	Literature
ZigBee Pro	N/A	−100	250 bps	< 100	100 ~ 500μW	N/A	ZigBee Alliance [82]
BLE 5	N/A	−97	1 ~ 2 Mbps	< 200	20 mW	0	Bluetooth SIG [83]
Sigfox	N/A	−142	1 ~ 100 bps (uplink)	> 10k	100 mW	14 dBm	Sigfox [84]
LoRa	N/A	−148	0.3 ~ 50 kbps	> 10k	150 mW	N/A	Semtech Corp. [85]
NB-IoT	N/A	−141	204.8 kbps (Uplink)	> 10k	500 mW	23 (UE)	Ratasuk *et al.* [86]
RFID (EPC-global Gen2)	N/A	−85	40 − 640 kbps	>10	1 ~ 10 μW	31.5	GS1 AISBL [87]

Aalto University
School of Electrical
Engineering

2. Basic principle

Backscatter communications

- Backscatter of radio waves from an object has been a subject of active study since the development of *radar* back in the 1930's, and the use of backscattered radio for communications since Harry Stockman's work in 1948.
- Backscatter Communications (BC) is widely used in RFID where a reader device generates an unmodulated carrier signal, a passive tag absorbs the energy of this signal and then sends back the modulated signal to the reader.
- BC devices do not need a power-hungry transceiver and can achieve up to 1000 times lower power consumption and 10 to 100 times lower device cost than contemporary active-transceiver-based solutions.

Ambient backscatter communications

- *Passive radar systems* encompass a class of radar systems that detect and track objects by processing reflections from non-cooperative sources of illumination in the environment, such as commercial broadcast and communications signals. It is a specific case of bistatic radar, the latter also including the exploitation of cooperative and non-cooperative radar transmitters.
- Passive radar is almost as old as radar with first experiments in UK in 1935.
- Ambient backscatter communications can be interpreted as a communication technology using the passive radar principle. Ambient backscatter was invented by researchers at University of Washington around 2013.

Liu, V., Parks, A., Talla, V., Gollakota, S., Wetherall, D. and Smith, J.R., 2013, August. Ambient backscatter: wireless communication out of thin air. In *ACM SIGCOMM Computer Communication Review* (Vol. 43, No. 4, pp. 39-50). ACM.

Backscatter communications

- Modulated backscatter systems (MBS)

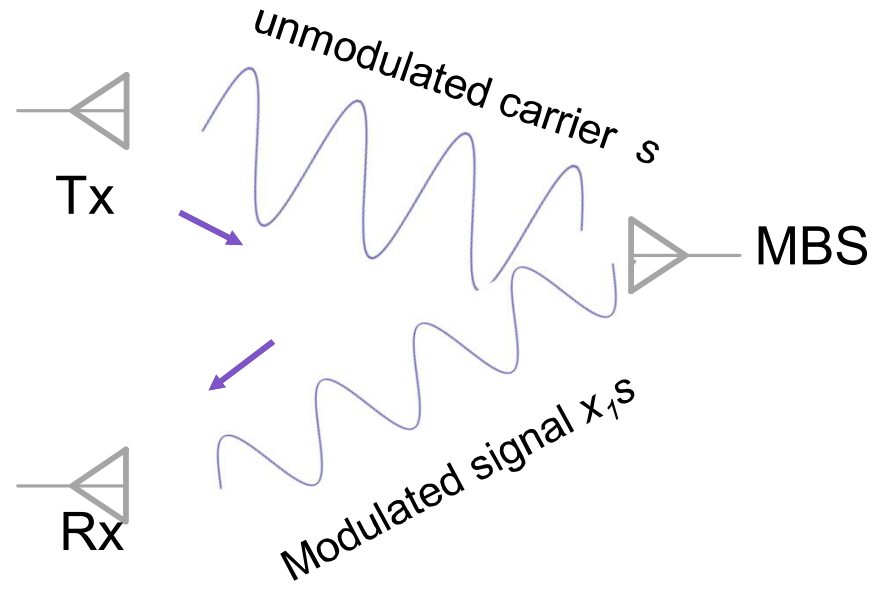

s equivalent base band carrier
x_1 complex reflection coefficient

Ambient backscatter communications

- Modulate ambient RF is modulated and reflected

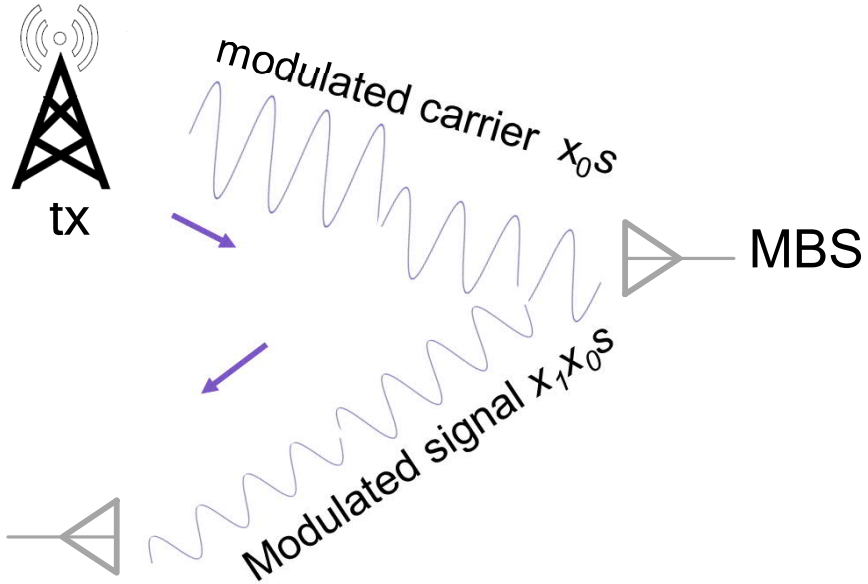

s equivalent base band carrier
x_0 symbol carried by the ambient RF
x_1 complex reflection coefficient

Ambient backscatter communications

- **Simple non-coherent transmit and receive strategies can be used for ultra-low power devices**

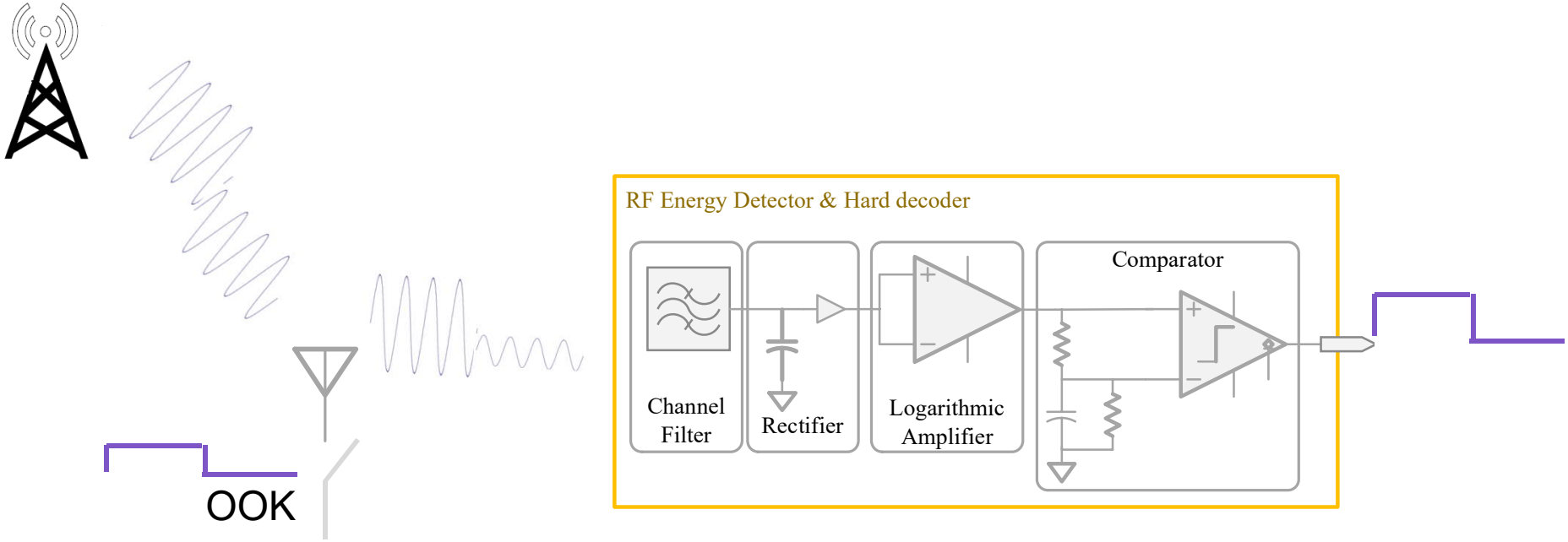

Bi-static modulated re-scatter system

- Can we decode both symbols x_0 and x_1? (Yes, we can)

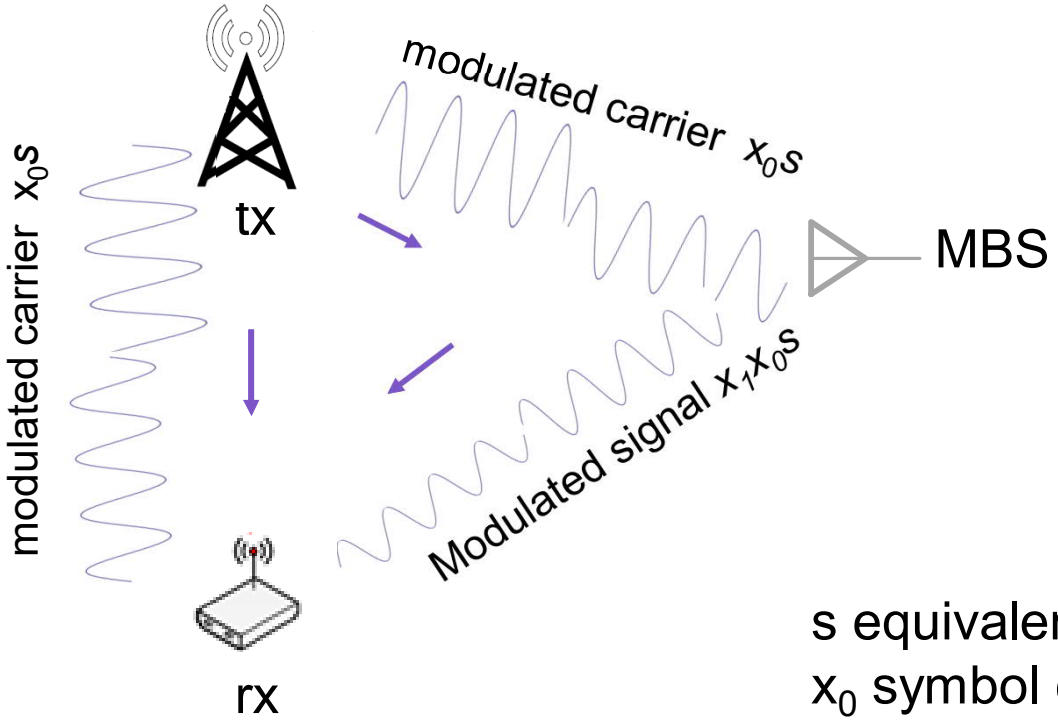

s equivalent base band carrier
x_0 symbol carried by the ambient RF
x_1 complex reflection coefficient

Ambient Backscatter Deployment options

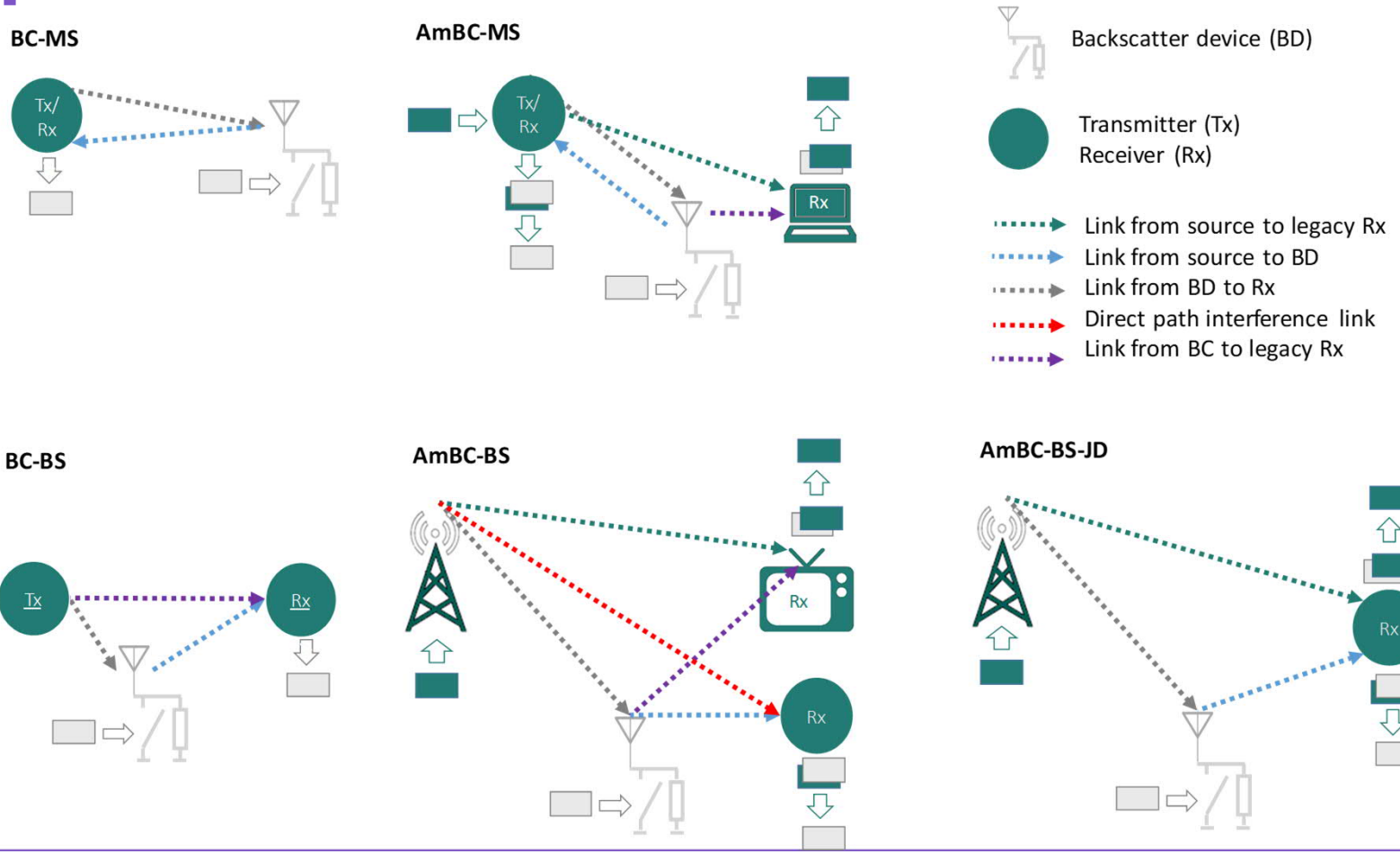

Aalto University
School of Electrical
Engineering

2. State-of-art and applications

Developed *backscatter* communication technologies

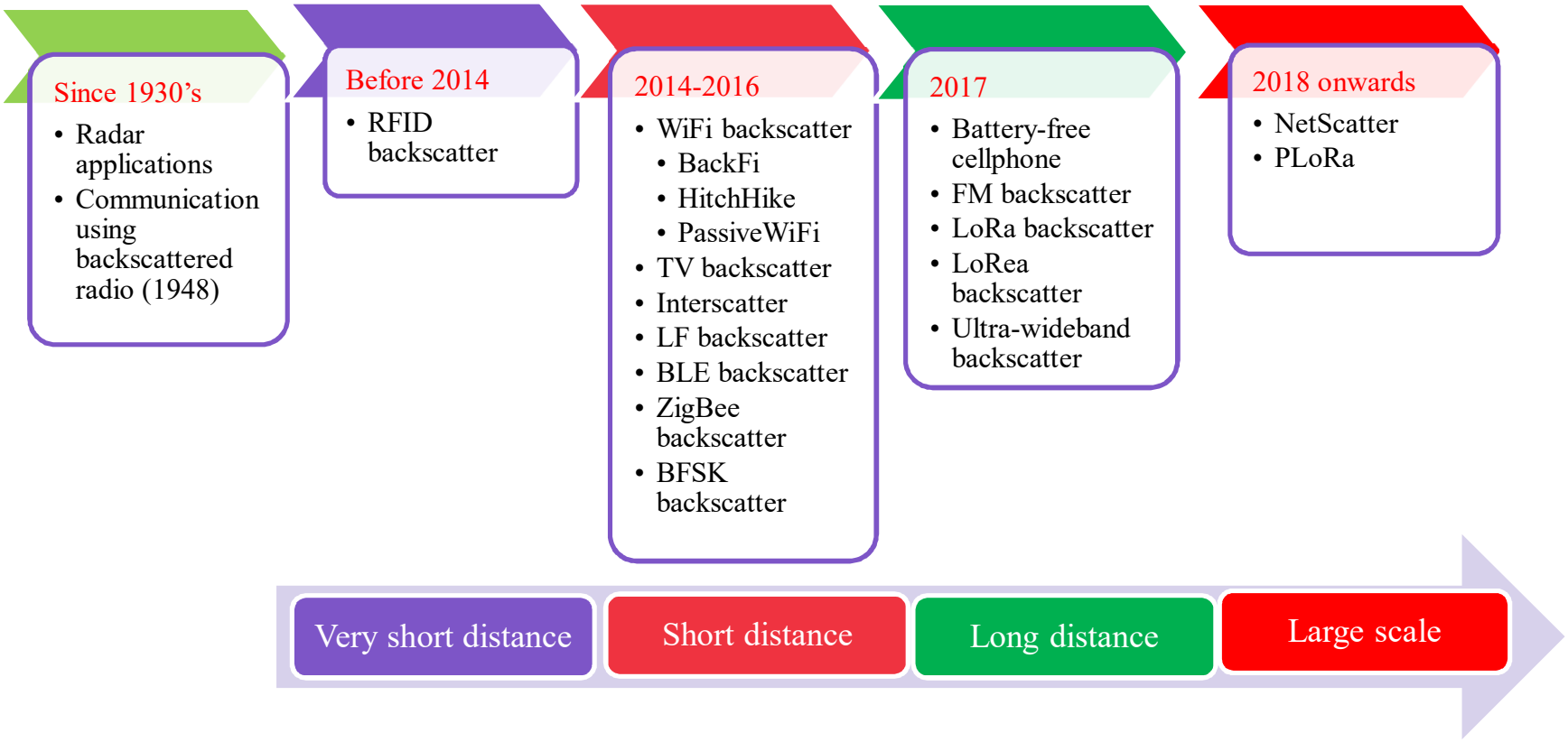

Aalto University
School of Electrical
Engineering

3. Modulation

Load modulation

- The backscattering device varies the complex antenna load reflection coefficient by switching the antenna load between states.

$$\Gamma = \frac{Z_L - Z_a^*}{Z_L + Z_a^*}$$

Γ : reflection coefficient,
Z_L: the antenna load impetence,
Z_a^* : the antenna impedance.

- Modulated backscatter can generate, for instance,
  - *Amplitude Shift Keying (ASK): resistive modulator impedance [Ishizaki et al. 2011]; OOK: Load modulator.*
  - *Frequency shift keying (FSK): digital [Vougioukas et al. 2016]; Frequency shifting: low-power ring oscillator-based clock generator [Zhang et al. 2016].*
  - *Phase shift keying (PSK), reactive modulator impedance in the Gen2 standard; transmission line for RFID .*
  - *Quadrature amplitude modulation (QAM).*

Simple backscatter modulators

- **On-off keying (OOK)**
  - Very wideband (limited by antenna)
  - 30 dB between on and off-state
- **Binary phase shift keying (BPSK)**
  - Wideband, but phase shift depend on the utilized frequency.

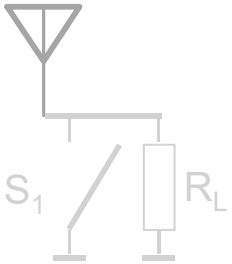

OOK modulator

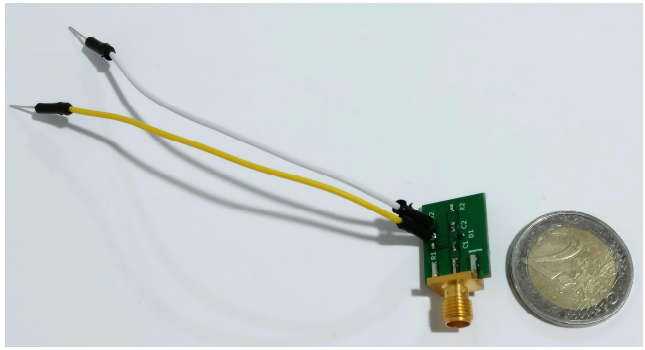

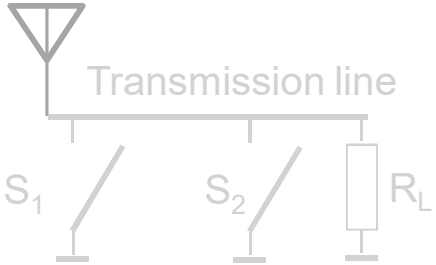

BPSK modulator

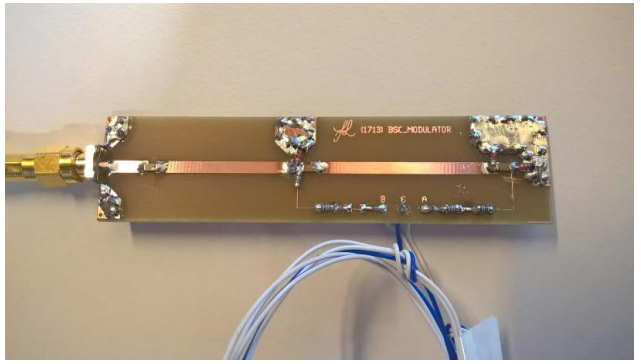

Backscatter modulation methods

A TABLE SUMMARIZES THE MODULATION TECHNIQUES BY THE PROTOTYPES.

Modulation	Modulator	Implementation	Power consumption	Literature
OOK	load modulator	RC-circuit	$< 30.8\mu$W	Ishizaki *et al.* [31]
OOK	load modulator	a switch to adjust the RCS of a patch antenna	1 μW	Kellogg *et al.* [27]
M-PSK	phase modulator	multiple RF single pole double throw switches connected in a binary tree structure	3.15 pJ/bit	Bharadia *et al.* [28]
QAM	load modulation	multi-state complex-valued modulation using single-chip CMOS	115 nW	Thomas *et al.* [96], [97]
FSK	field effect transistor	a combination of fundamental- and harmonic-mode subcarrier modulation	28.4 pJ/bit	Ensworth *et al.* [12]
BFSK	load modulation	single RF switching transistor	N/A	Vougioukas *et al.* [92]
analog FM	RC components	RC-circuit and a timer	1.5 mW	Kampianakis *et al.* [69], [98]
fixed FS and OOK	data modulator	ring oscillator-based clock generator and RF transistor	45 μW	Zhang *et al.* [21]

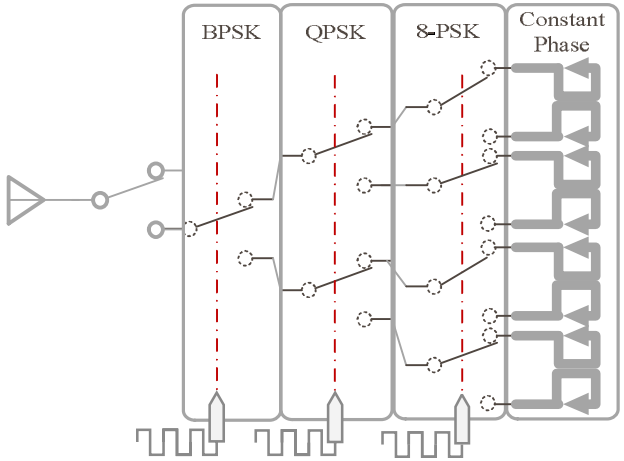

Backscatter modulation with reflection amplification

A backscatter device with reflection amplifier is similar to amplify and forward relay except in addition to amplifying the signal it also modulates the amplified signal.

Packet level modulation

WiFi backscatter [Kellogg *et al.* 2014]: encodes a bit ‘1’ when the WiFi packets are present, otherwise it encodes a bit ‘0’ (silence period); the tag receiver detects the different periods of the WiFi packets using an energy detector. To avoid other readers to transmit during the silence period, the reader needs to send a CTS_to_SELF packet before transmitting encoded information.

Kellogg, B., Parks, A., Gollakota, S., Smith, J.R. and Wetherall, D., 2014, August. Wi-Fi backscatter: Internet connectivity for RF-powered devices. In *ACM SIGCOMM Computer Communication Review* (Vol. 44, No. 4, pp. 607-618). ACM.

Waveform designs for AmBC

- Line codes
- Spread spectrum techniques
  - Direct sequence spread spectrum (DSS)
    - *Perfect pulses*
  - Chirp spread spectrum (CSS)
    - *Lora backscatter: Generate LoRa waveform*
    - *Netscatter: Chiprs + OOK*

Perfect pulses

- Based on antipodal binary waveform
- DC-nulling that the intra-symbol transitions can remove $f^{2(n-1)}$ frequency components in the pulse's power spectrum.
- Generating the waveforms: the transitions are produced by

$$\tau_i = -\frac{1}{2}\cos\left(\frac{i\pi}{n+1}\right), \quad \forall\, i = 0,\cdots,n, \text{ where } \tau_0 = -\frac{1}{2} \text{ and } \tau_n = \frac{1}{2}.$$

- These waveforms have been used for BPSK, FSK, and pulse width modulation (PWM) modulations.

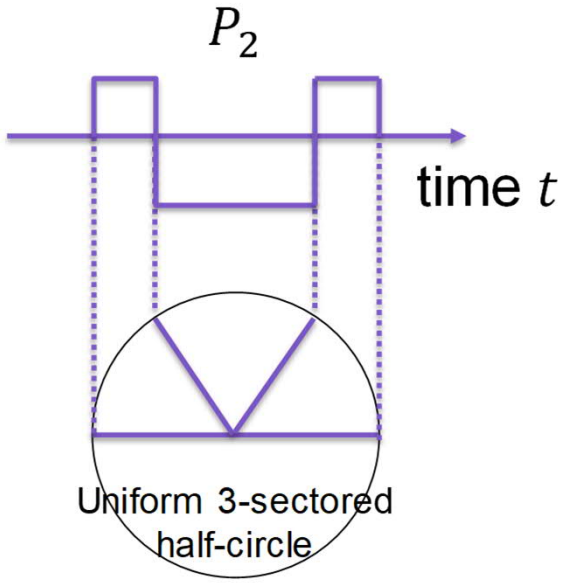

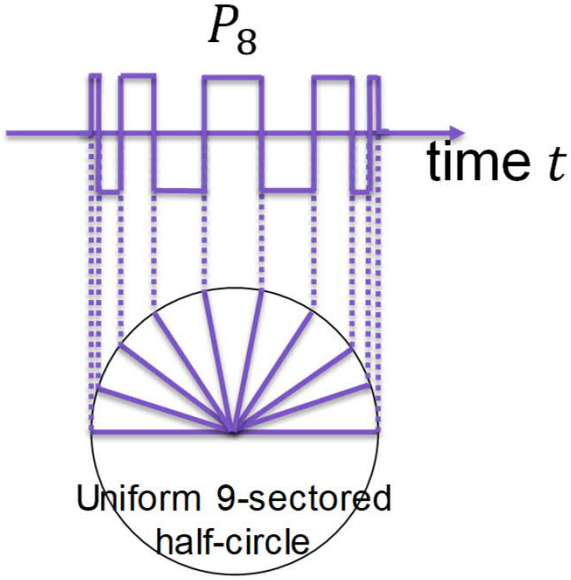

Varner, M.A., Bhattacharjea, R. and Durgin, G.D., 2017, May. Perfect pulses for ambient backscatter communication. In *2017 IEEE International Conference on RFID (RFID)* (pp. 13-19). IEEE.

Perfect pulses

- Incorporated modulated waveforms and perfect pulse P_n

P_4 –BPSK

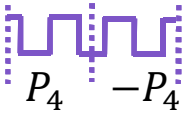

P_4P_8 –FSK

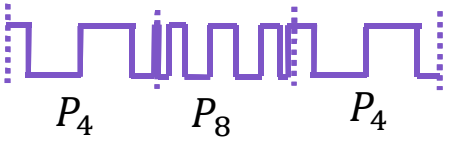

P_4 –PWM

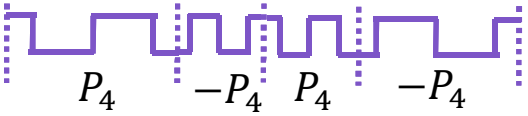

Chirp Pulses

[Talla2017 Peng *et al.* 2018, Hessar *et al.* 2019]

- Chirp spectrum spread (CSS) modulation technique uses chirp pulses to convey information.
- Principles: A time delay in the chirp signal translates to a frequency shift.
- Advantage: improving the spectral efficiency by canceling the sideband harmonics.
- Synchronization of the slots across different backscatter devices: using a unique ON-OFF keying *sync pattern* at the beginning of the TDMA round robin. This allows devices to determine the slot boundaries for a whole round-robin duration.

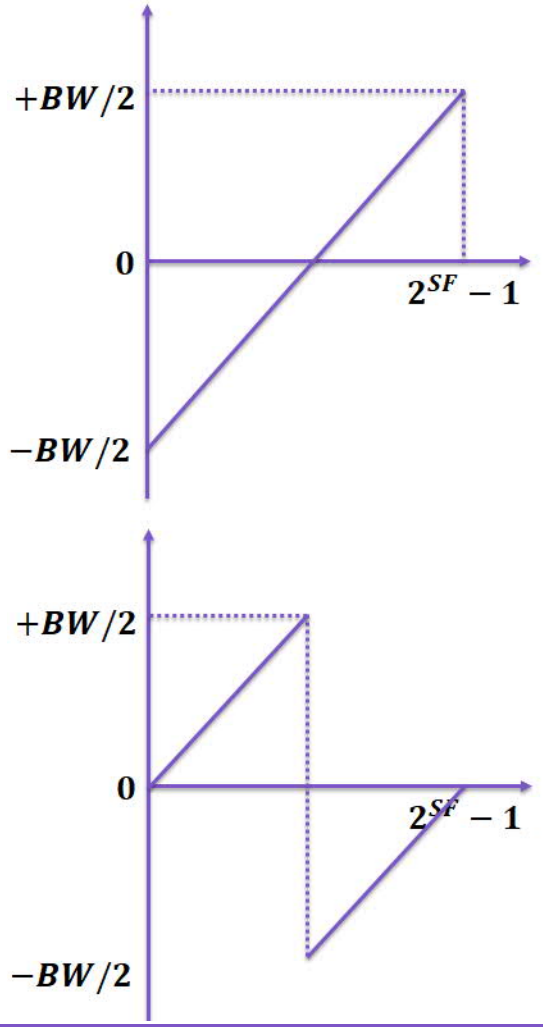

Aalto University
School of Electrical
Engineering

5. Propagation

Propagation

Backscatter communications link budget in bi-static case:

$$P_R = \frac{P_T G_T G_R G_{BC}^2 \lambda^4 X_f X_{BC} M}{(4\pi)^4 r_f^2 r_{BC}^2 \Theta^2 B_f B_{BC} F_{BDBCS}},$$

P_R	Received power
P_T	Transmit power
G_T	Transmitter antenna gain
G_R	Receiver antenna gain
G_{BC}	BC antenna gain
Λ	wavelength
X_f	Forwardlink polarization mismatch
X_{BC}	BC link polarization mismatch
r_f	Forward link distance
r_{BC}	BC link distance
B_f	Forward link blockage (shadow fading)
B_{BC}	BC link blockage
M	BC modulation loss
Θ	On-object penalty
F_{BDBCS}	Fade margin

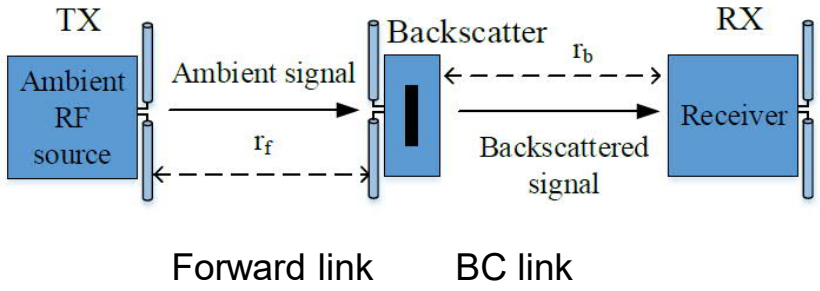

Propagation

Measurement setup:

f =	590 MHz	Digital TV band
P_T =	10 dBm	Tx power
$G_T=G_R=G_{BC}$	0 dBi	Isotropic antennas
M =	-6.63 dB	Modulator factor at the tag

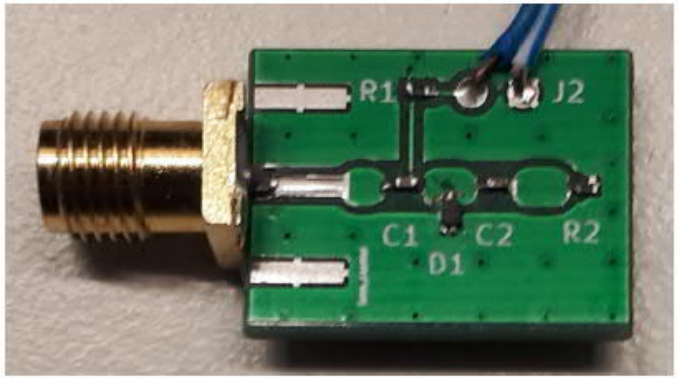

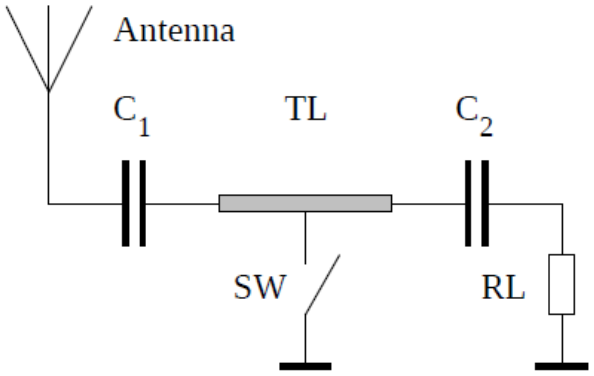

Badihi B, Liljemark A., Sheik. M. U., Lietzen J., Jäntti R. "Link Budget Validation for Backscatter-Radio System in Sub-1GHz" submitted to IEEE WCNC 2019

Propagation

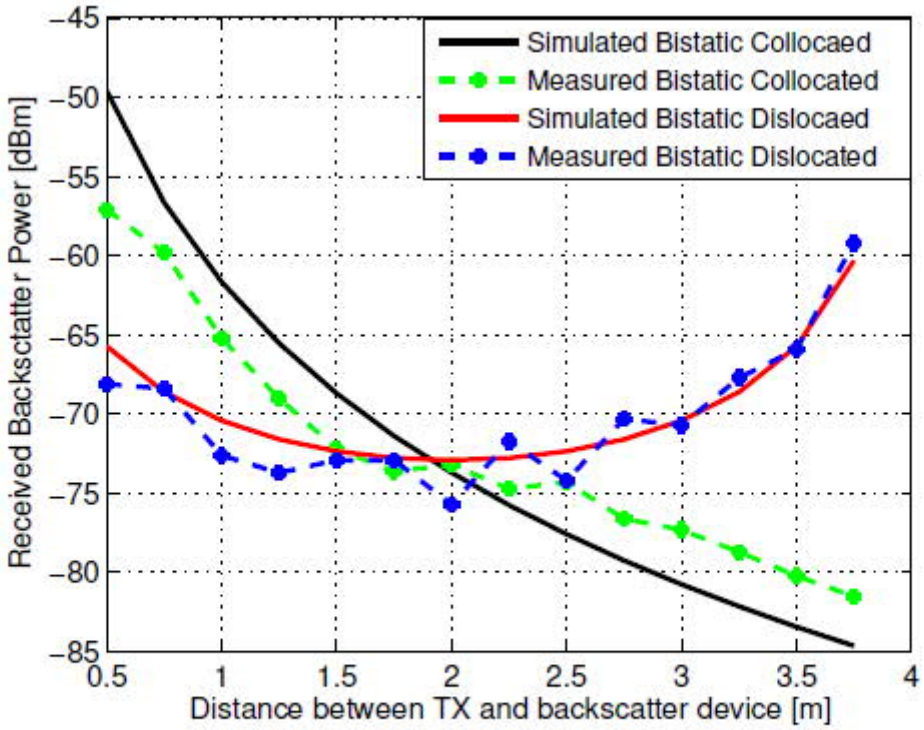

Fig. 5. Measured and simulated backscatter power in anechoic chamber.

Propagation

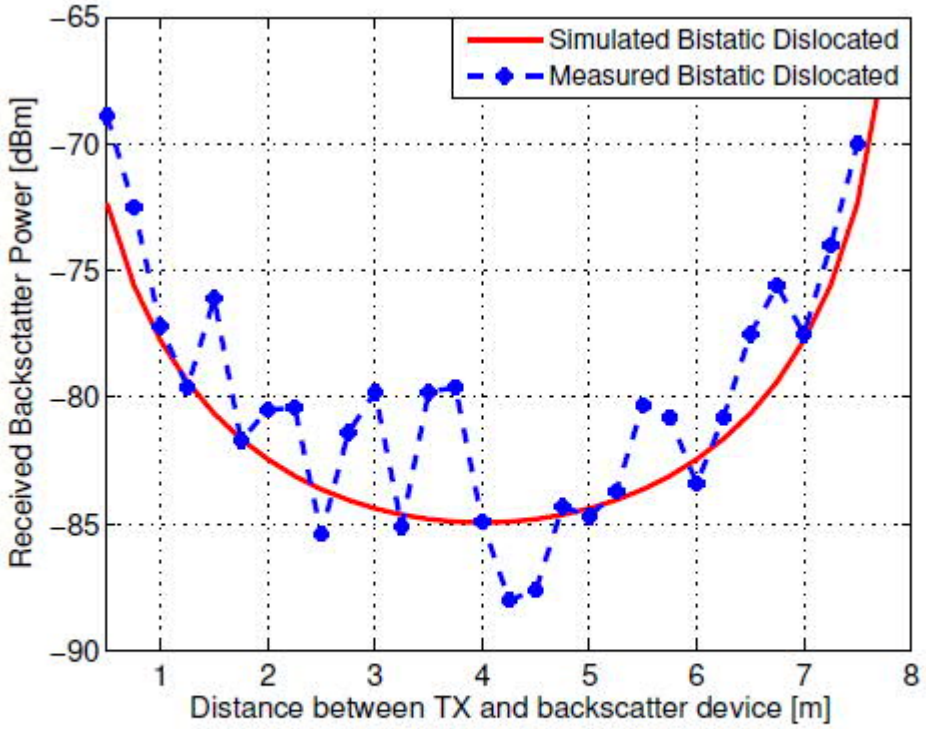

Fig. 6. Measured and simulated backscatter power in office corridor.

Propagation

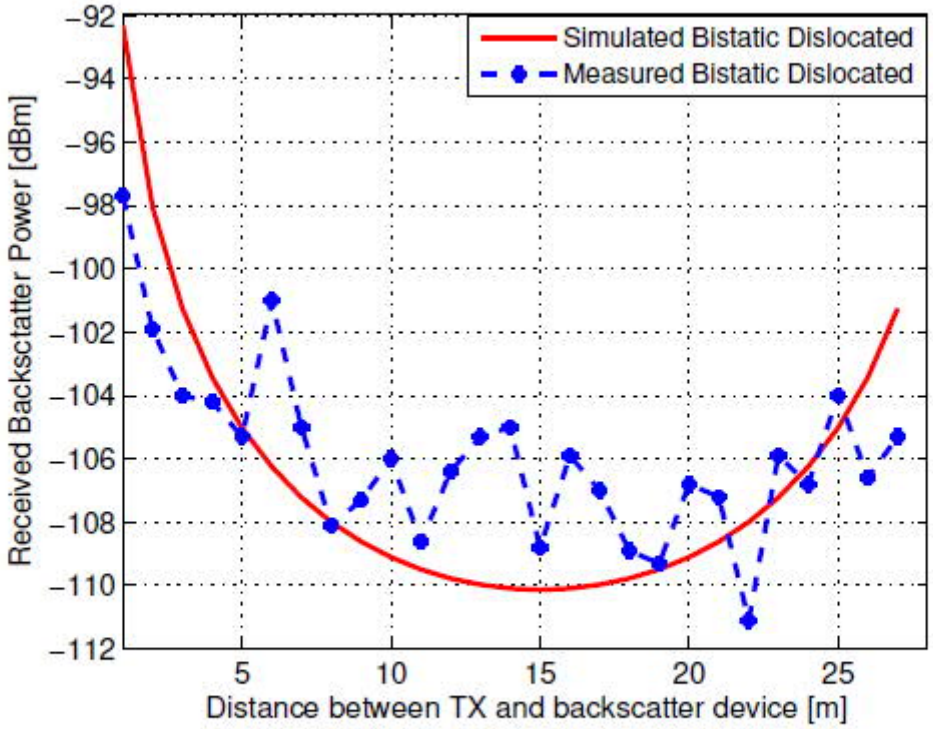

Fig. 7. Measured and simulated backscatter power in outdoor environment.

Propagation

Scattering link gain

$$g_s = \left(\frac{\lambda}{4\pi r_1}\right)^2 \left(\frac{\lambda}{4\pi r_2}\right)^2$$

Reflection link gain

$$g_r = \left(\frac{\lambda}{4\pi(r_1 + r_2)}\right)^2$$

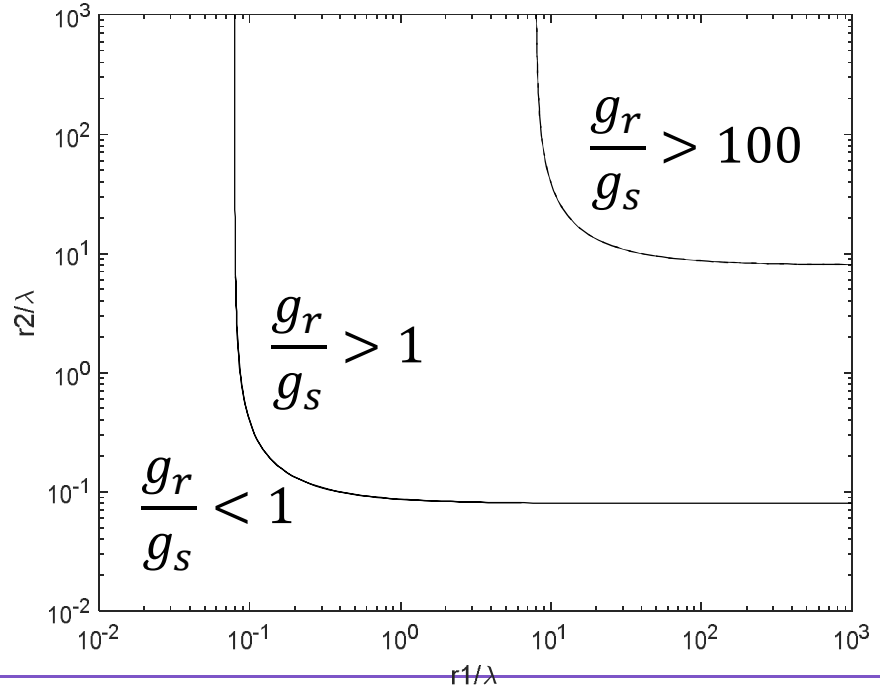

Fading

- Backscatter radio systems operate in the dyadic backscatter channel: product of the forward and backscattered channel.
- Both links can experience fading.
- Depending on the environment, this fading can be either correlated or uncorrelated.

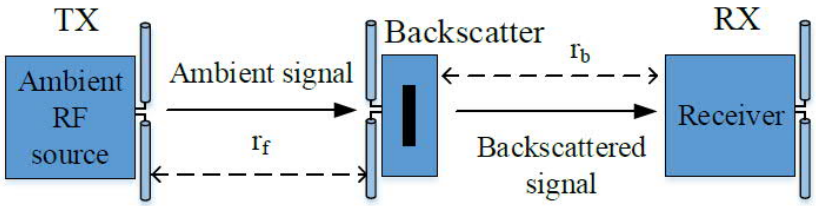

- Also the amplitude variation of the ambient signal appear as fading fort the AmBC receiver.

Fading

Fading marginal for Nagagami – Nagagami and Rayleigh-Nagagami-Nagagami channels

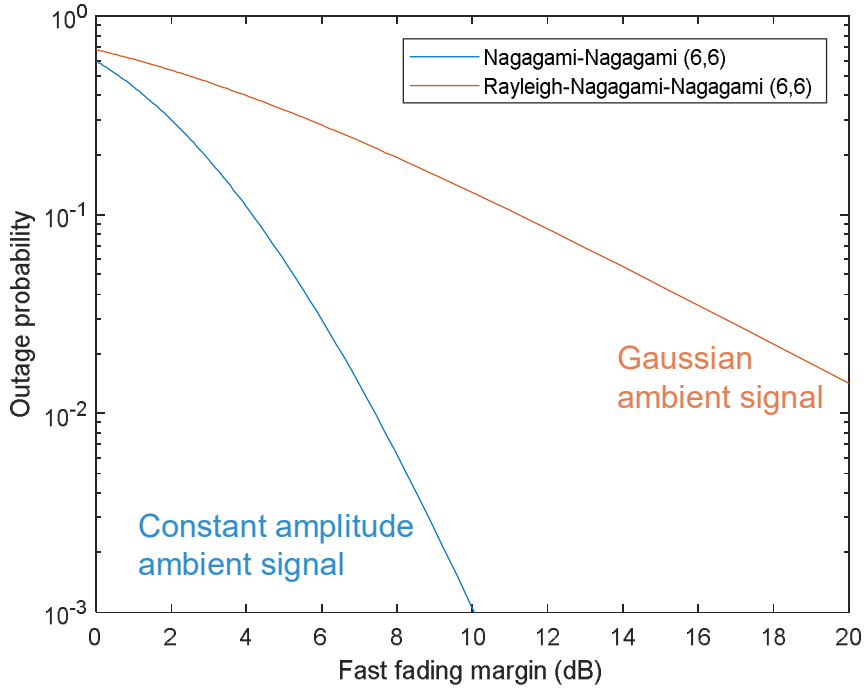

Aalto University
School of Electrical
Engineering

6. Mitigating direct path interference at the receiver

Dynamic range problem (1/2)

λ	Wavelength
G_m	MBS antenna gain
M	MBS modulation loss
SNR_0	Direct path SNR
SNR_1	Scattered path SNR

$$\frac{SNR_1}{SNR_0} = \left(\frac{\lambda}{4\pi}\right)^2 M{G_m}^2 \frac{{D_0}^2}{{D_1}^2{D_2}^2}$$

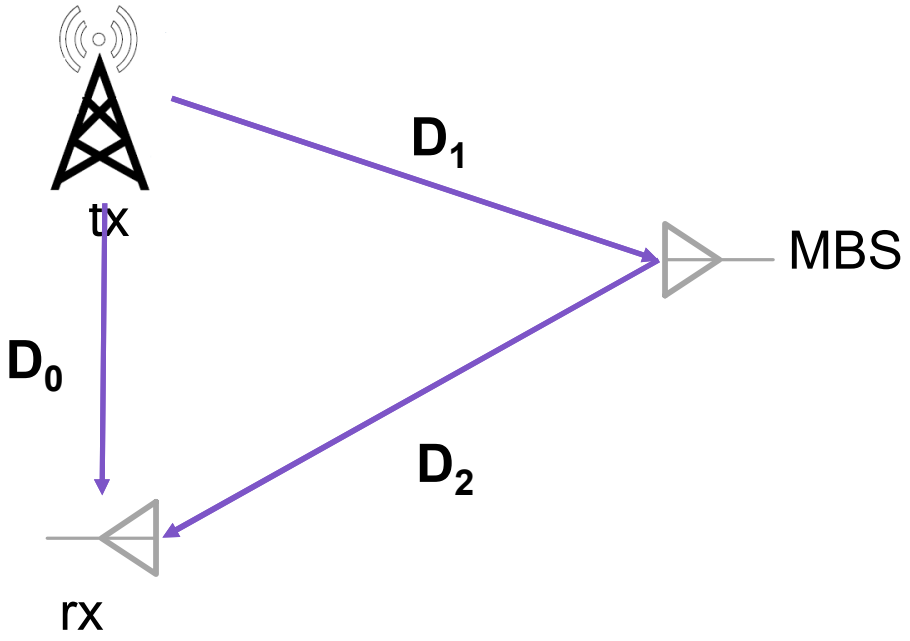

Dynamic range problem (2/2)

λ = 3 m (FM band)

G_m = 0 dB

M = 0 dB

SNR_0 = 50 dB

$$\frac{SNR_1}{SNR_0} = \left(\frac{\lambda}{4\pi}\right)^2 M {G_m}^2 \frac{{D_0}^2}{{D_1}^2 {D_2}^2}$$

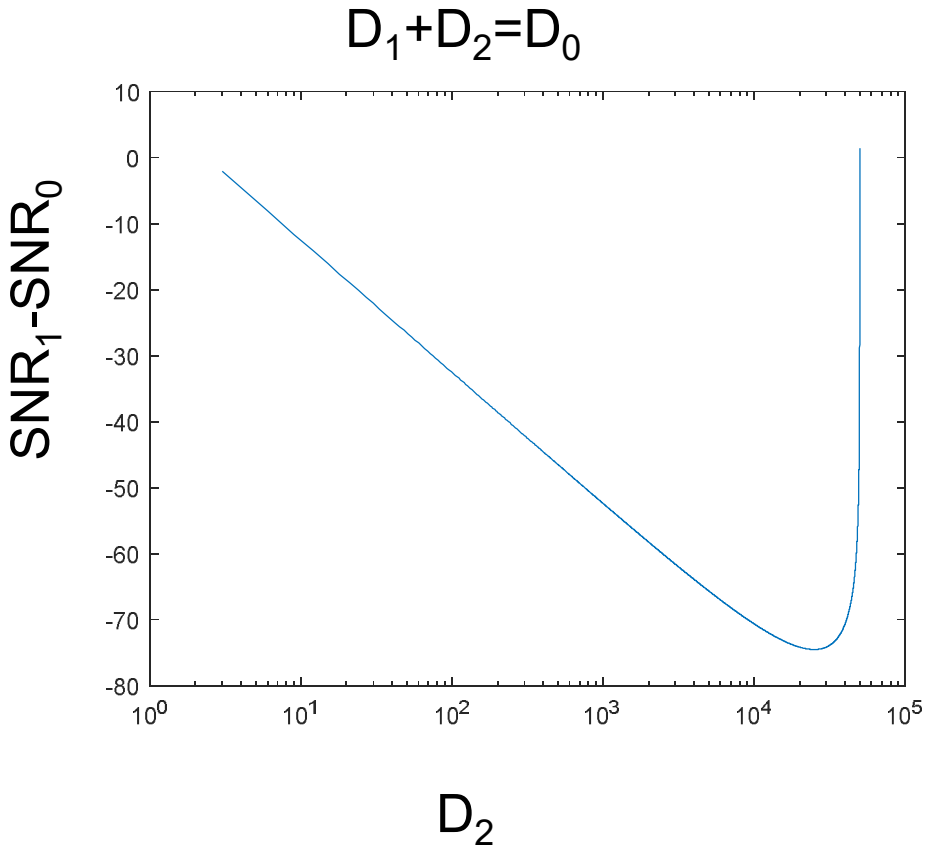

Required dynamic range is a limiting factor

Direct path interference

- **Received signal**

$$y=(h+g_r g_t x_1)x_0 + z$$
$$=(g_r g_t x_0)x_1 + (hx_0+z)$$

Fading

Interference + noise

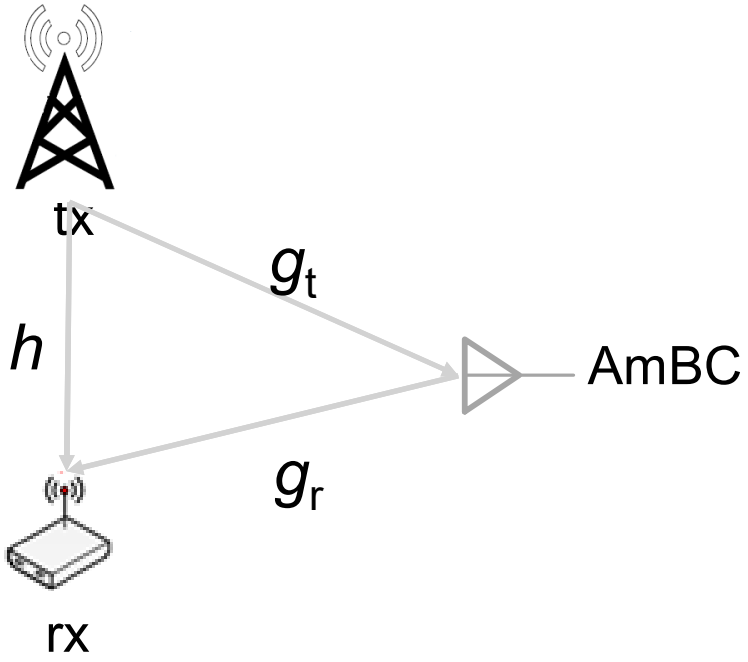

h direct path (complex channel gain)
g_t signal path from tx to AmBC
g_r signal path from AmBC to rx
x_0 symbol carried by the ambient RF
x_1 complex reflection coefficient

Impact of direct path interference

$x_0 \sim CN(0,1)$ Complex Gaussian ambient signal

$x_1 \in \{0,1\}$ AmBC uses on-off-keying

$$y|x_1 \sim CN(0, |h_0|^2 + |g_0 g_1|^2 x_1 + \sigma_z^2)$$

Hypotehesis testing

H0: $y \sim CN(0, |h_0|^2 + \sigma_z^2)$

H1: $y \sim CN(0, |h_0|^2 + |g_0 g_1|^2 + \sigma_z^2)$

Direct path interference

Bit error probability for On-off-keying

AWGN channel with Complex Gaussian ambient signal

In order to improve range, the impact of direct path should be mitigated.

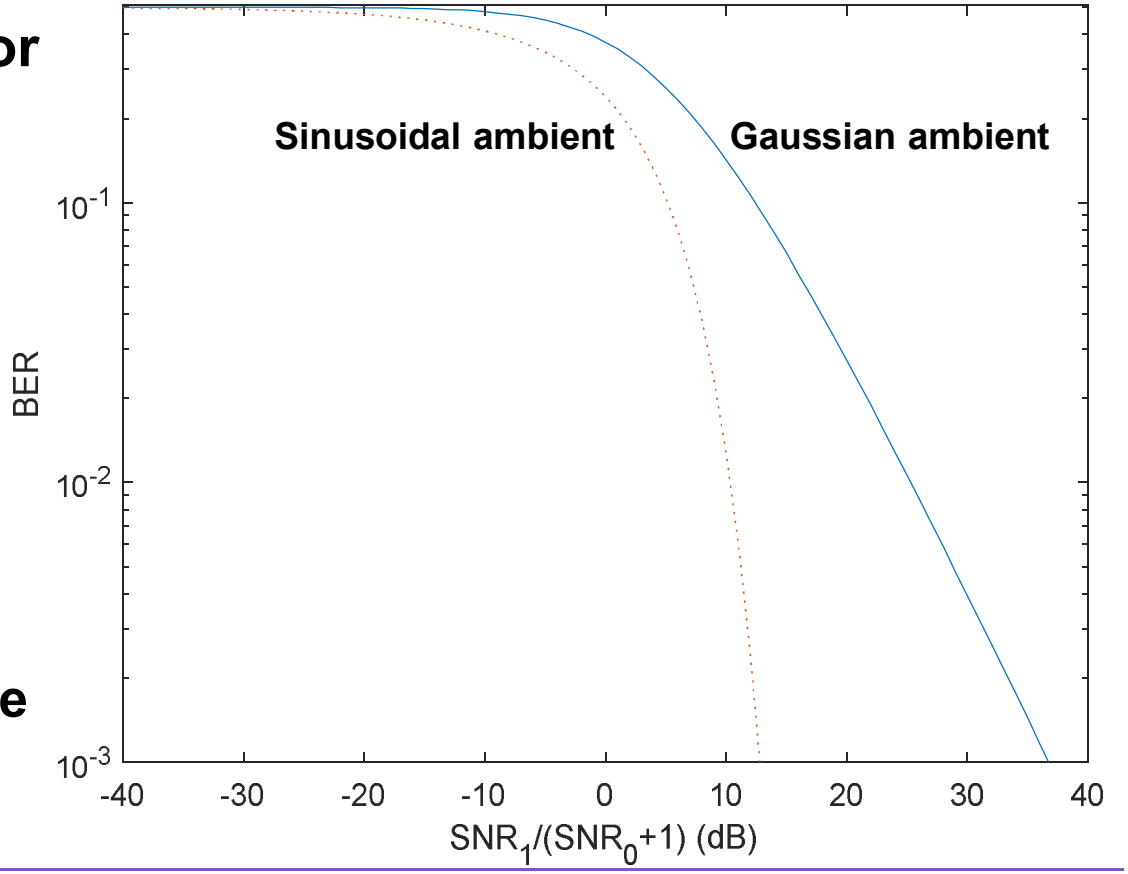

Direct path interference mitigation

1. Time domain approach
2. Frequency domain approach
3. Spatial domain approach
4. Signal processing approach

Time domain approach

MBS uses on – off keying (OOK) with long symbols
=> Time domain averaging

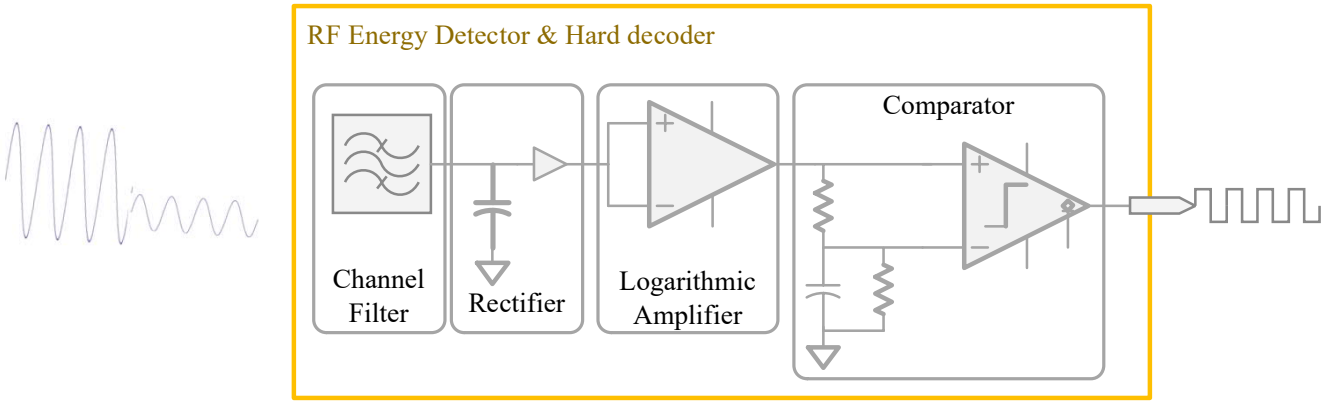

Frequency domain approach 1

Shift the spectrum of the scattered path in frequency domain

$$Y(f)=H(f)X_o(f) + G_r(f)\{X_1(f)*[G_t(f)X_o(f)]\} + Z(f)$$

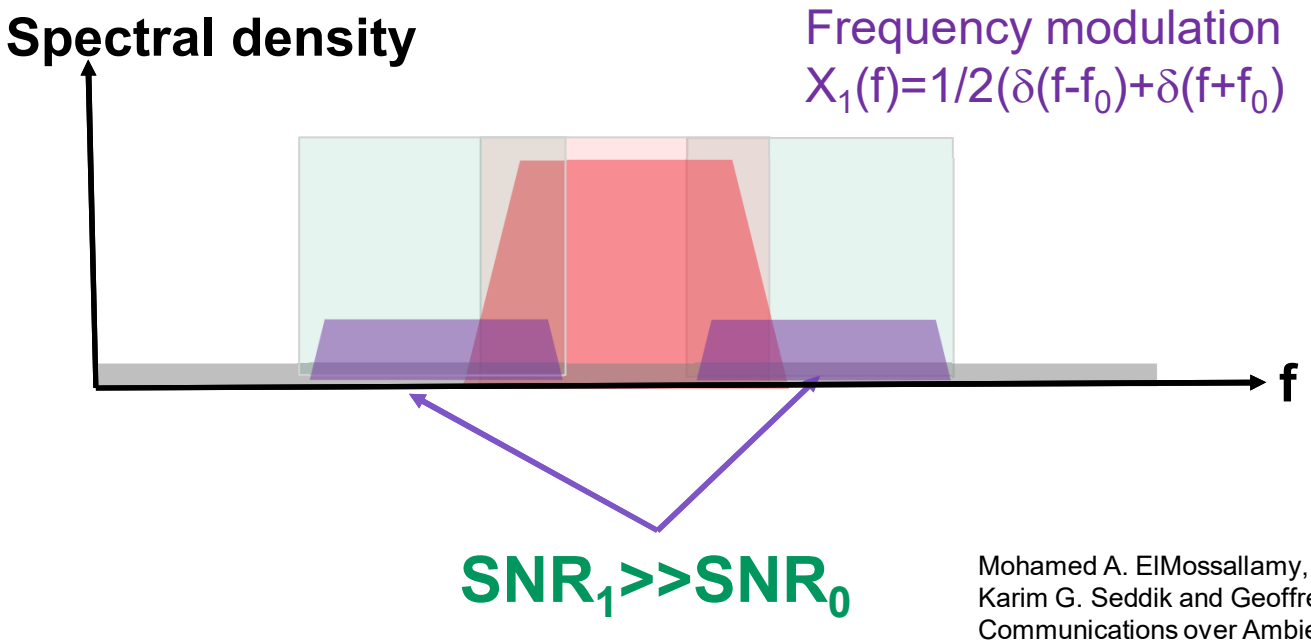

Mohamed A. ElMossallamy, Zhu Han, Miao Pan, Riku Jäntti, Karim G. Seddik and Geoffrey Ye Li, " Backscatter Communications over Ambient OFDM Signals using Null Subcarriers " 2018

Frequency domain approach 1

Direct path (FM signal)

FPGA generating sinusoidal wavefrom using pulse width modulation

Backscattered signal

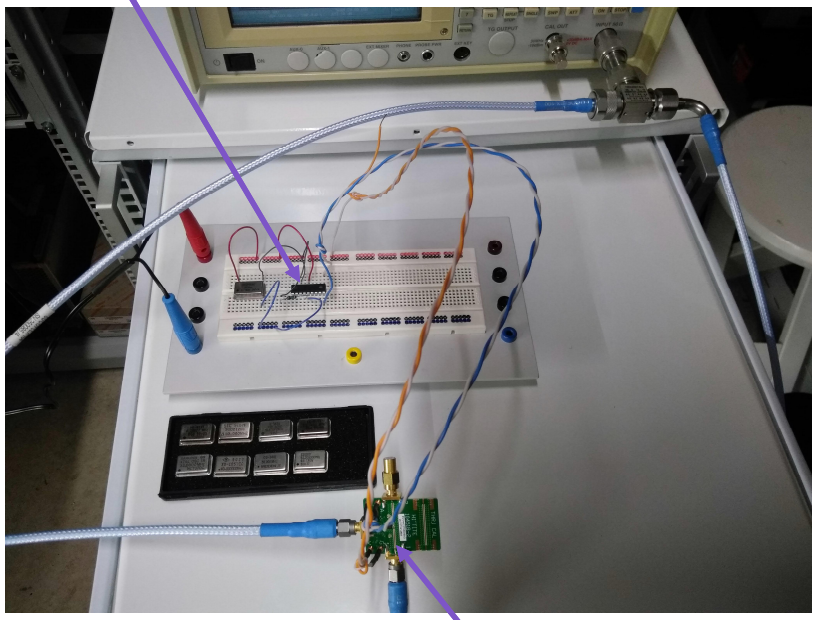

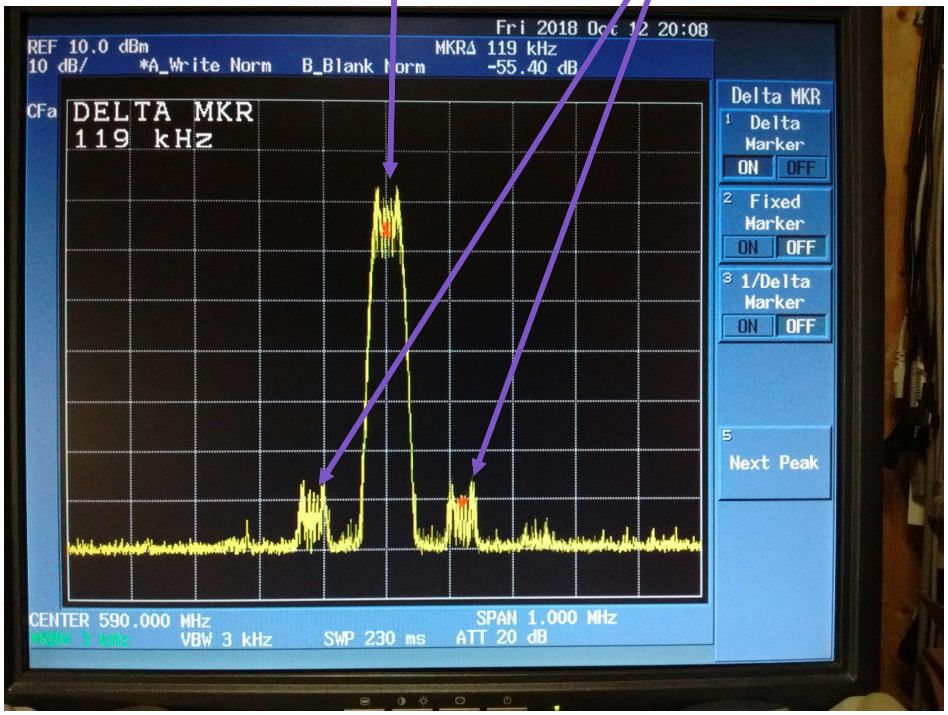

AmBC modulator

Frequency domain approach 2

Frequency shift keying

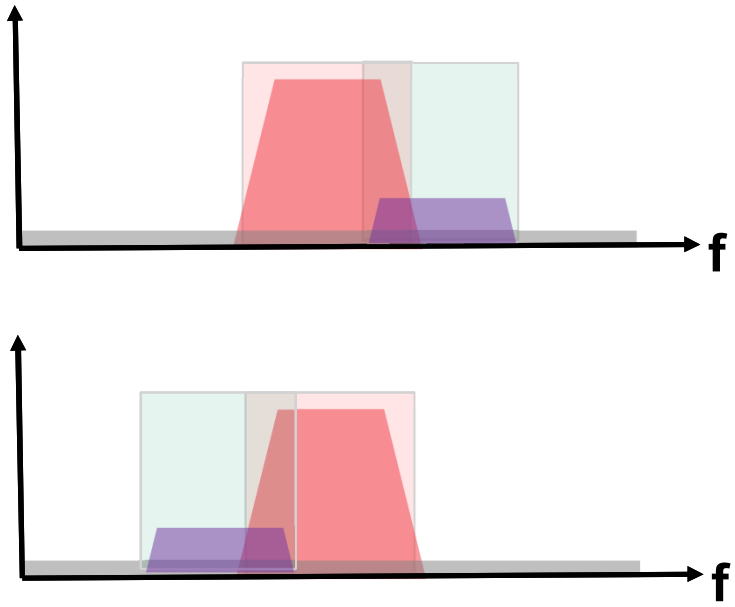

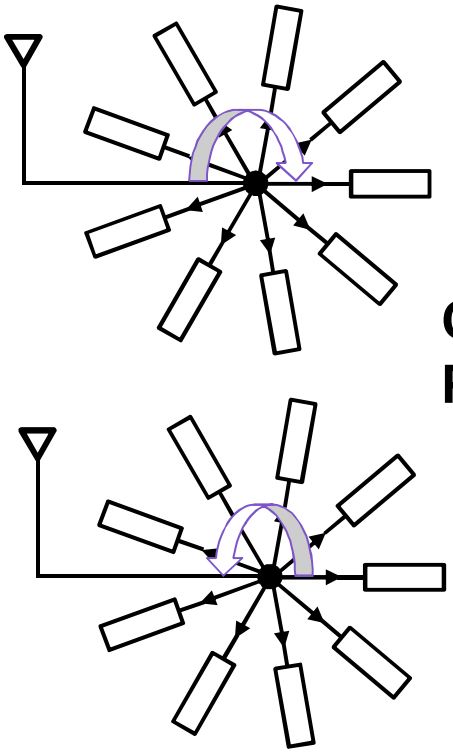

Cycle through Phase shifters

El Mossallamy, M.A., Pan, M., Jäntti, R., Seddik, K.G., Li, G.Y. and Han, Z., 2019. Noncoherent Backscatter Communications over Ambient OFDM Signals. *IEEE Transactions on Communications*

Frequency domain approach 2

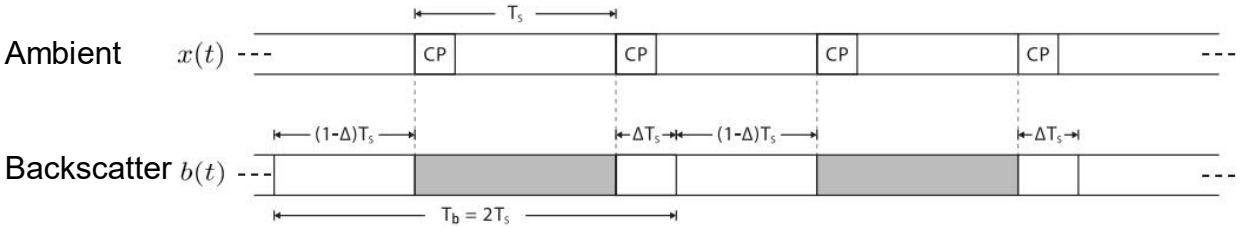

Fig. 11. Timing diagram for asynchronous tag operation. $\Delta \in (0, 1)$ denotes where the OFDM symbol overlaps with the tag symbol.

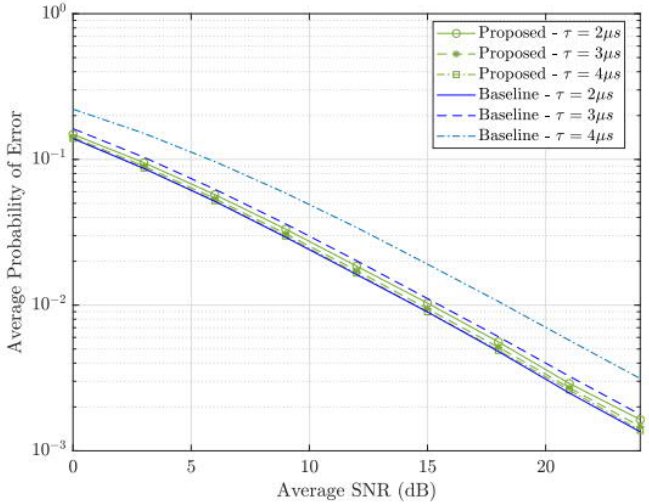

Fig. 4. Average probability of error for different values of maximum channel delay spread. Lines correspond to Monte-Carlo simulations and markers correspond to analytical expressions. Baseline scheme from [26]. $N_f = 1024, N_{cp} = 72, |\mathcal{U}| = 66, L_g = 1$.

$|\mathcal{U}|$ Number of inband null sub-carriers

N_f FFT block size

N_{cp} Cyclic prefix length

Frequency domain approach 3

- AmBC spreads part of the legacy signal
- Receiver performs dispreading which spreads the direct path signal

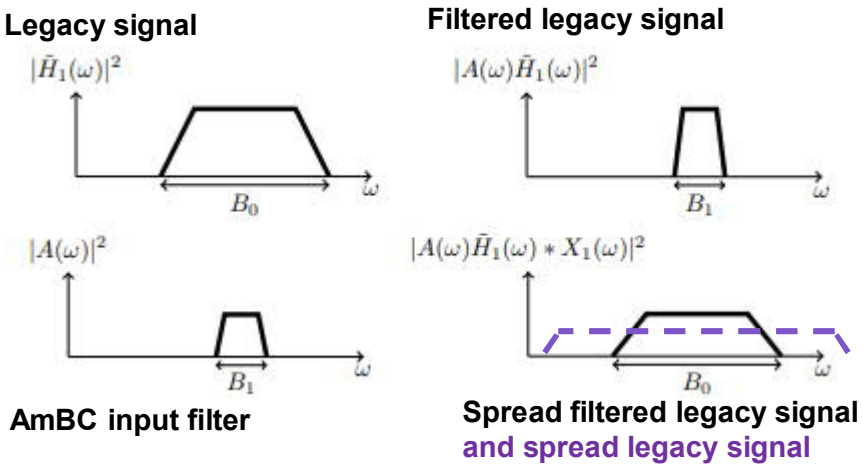

R. Duan, R. Jantti, M. ElMossallamy, Z. Han and M. Pan, "Multi-Antenna Receiver for Ambient Backscatter Communication Systems," *2018 IEEE 19th International Workshop on Signal Processing Advances in Wireless Communications (SPAWC)*, Kalamata, 2018, pp. 1-5.

Spatial domain approach 1

μmo two antenna receiver for on-off key modulated signal

Antenna outputs

$$|y_1(t)| = |h_{rf}s(t) + h_bB(t)s(t)|$$
$$|y_2(t)| = |h'_{rf}s(t) + h'_bB(t)s(t)|$$

Amplitude ratio

$$\frac{|y_1(t)|}{|y_2(t)|} = \frac{|h_{rf} + h_bB(t)|}{|h'_{rf} + h'_bB(t)|}$$

h_{rf} direct path link
h_b backscatter linl
s(t) ambient signal
b(t) backscatter signal

Parks, A.N., Liu, A., Gollakota, S. and Smith, J.R., 2015. Turbocharging ambient backscatter communication. *ACM SIGCOMM Computer Communication Review*, *44*(4), pp.619-630.

Spatial domain approach 2

Null steerign

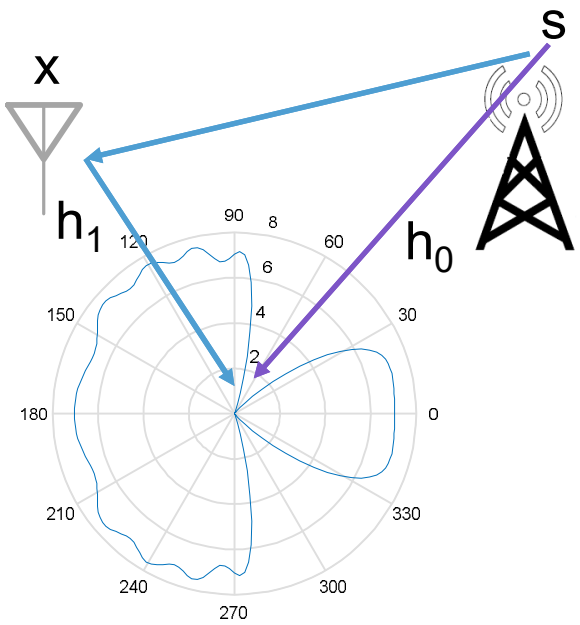

Null steering with 8 antenna receiver

R. Duan, E. Menta, H. Yigitler, R. Jäntti and Z. Han, "Hybrid Beamformer Design for High Dynamic Range Ambient Backscatter Receivers" Sumbitter 2019
https://arxiv.org/abs/1901.05323v2

Spatial domain approach 2

Two antenna testbed

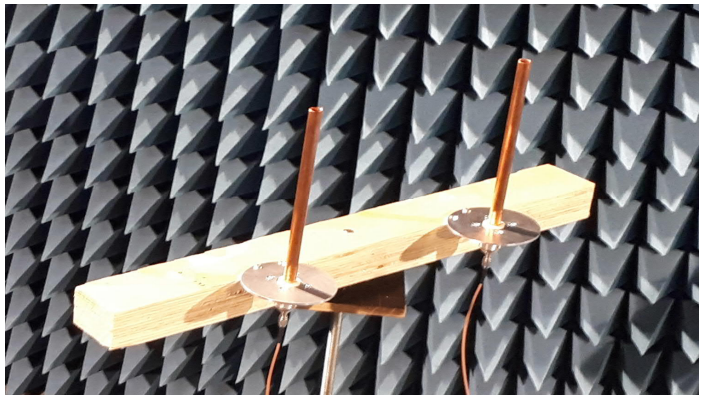

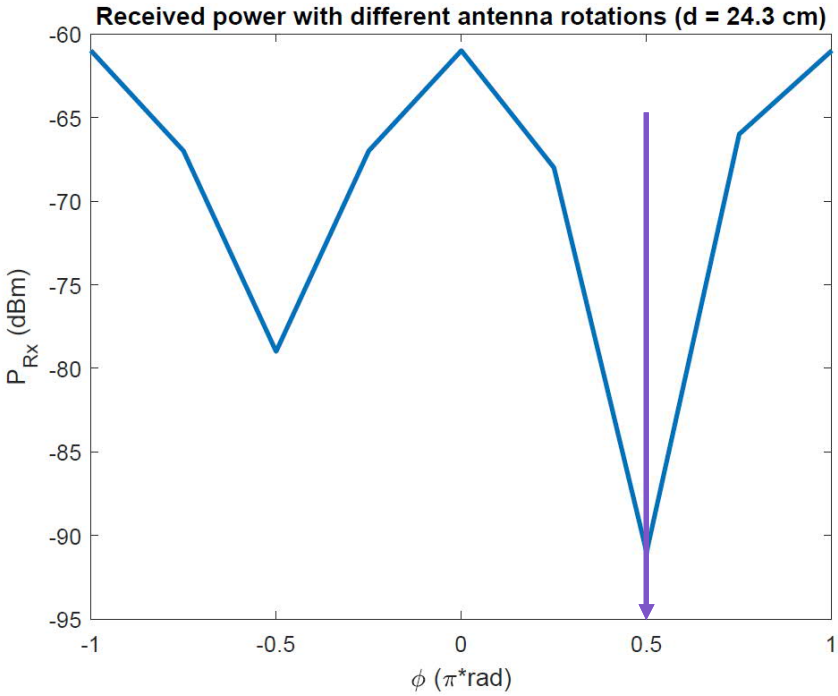

Theoretically -∞ dB
In practice ≈-30 dB

Spatial domain approach 2

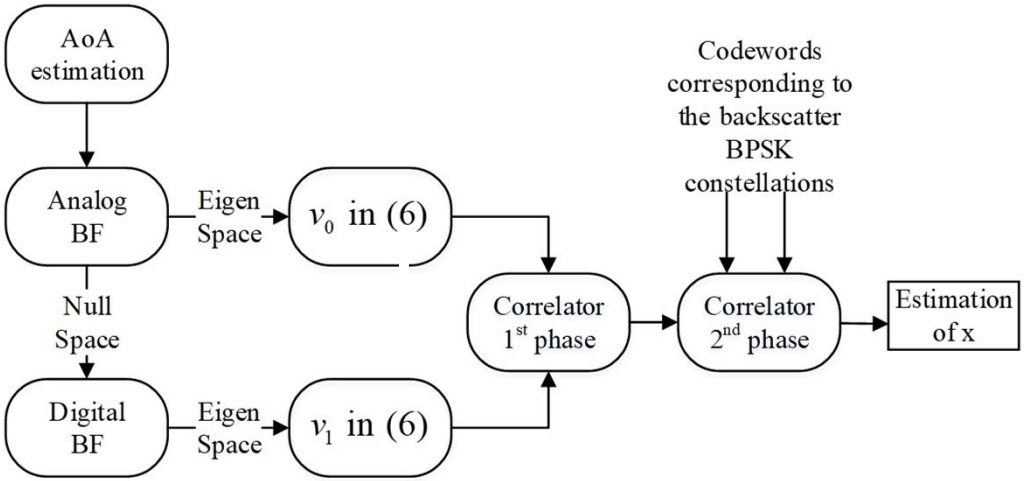

Two stage beam-former

unknown phase of the ambient signal is removed

Beam-former outputs

$$v_0[i] \approx h_0 s[i] + \zeta_0[i],$$
$$v_1[i] = h_1 s[i]\tilde{x}[i] + \zeta_1[i], \quad \forall i = 1, \cdots, M,$$

Cross-correlation

$$\tilde{r}[i] = v_0[i]^* v_1[i] = h_0^* h_1 |s[i]|^2 \tilde{x}[i] + \tilde{\zeta}[i],$$

Direct path interference is nulled

Spatial domain approach 2

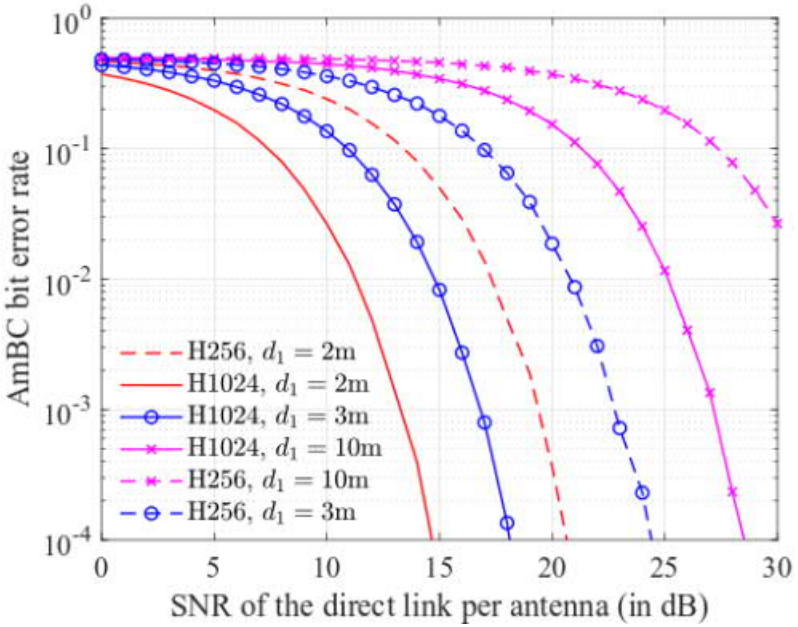

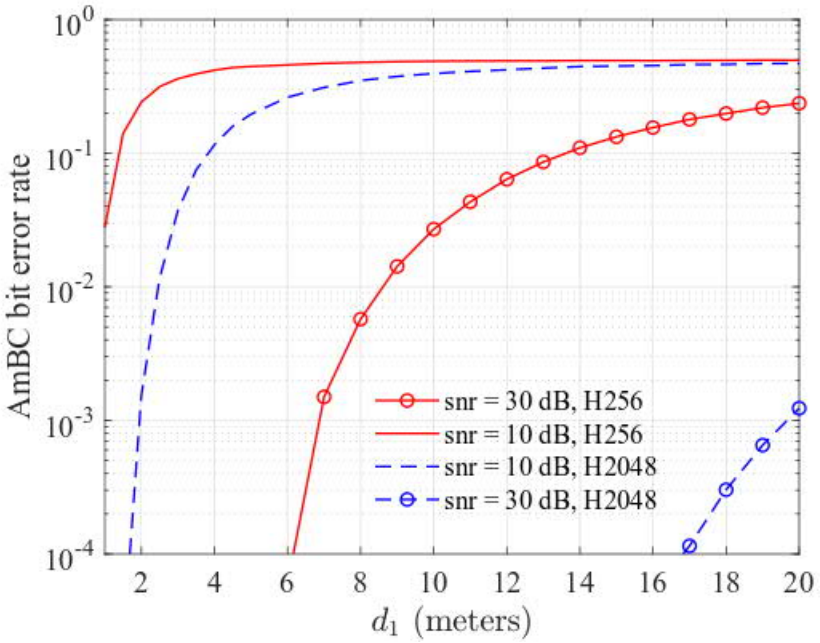

Carrier frequency: 500 MHz; receive antenna array has 8 elements; AoA estimation is carried out using the Bartlett method; H_M denotes a length-*M* Hadamard codeword.

Polarization domain approach

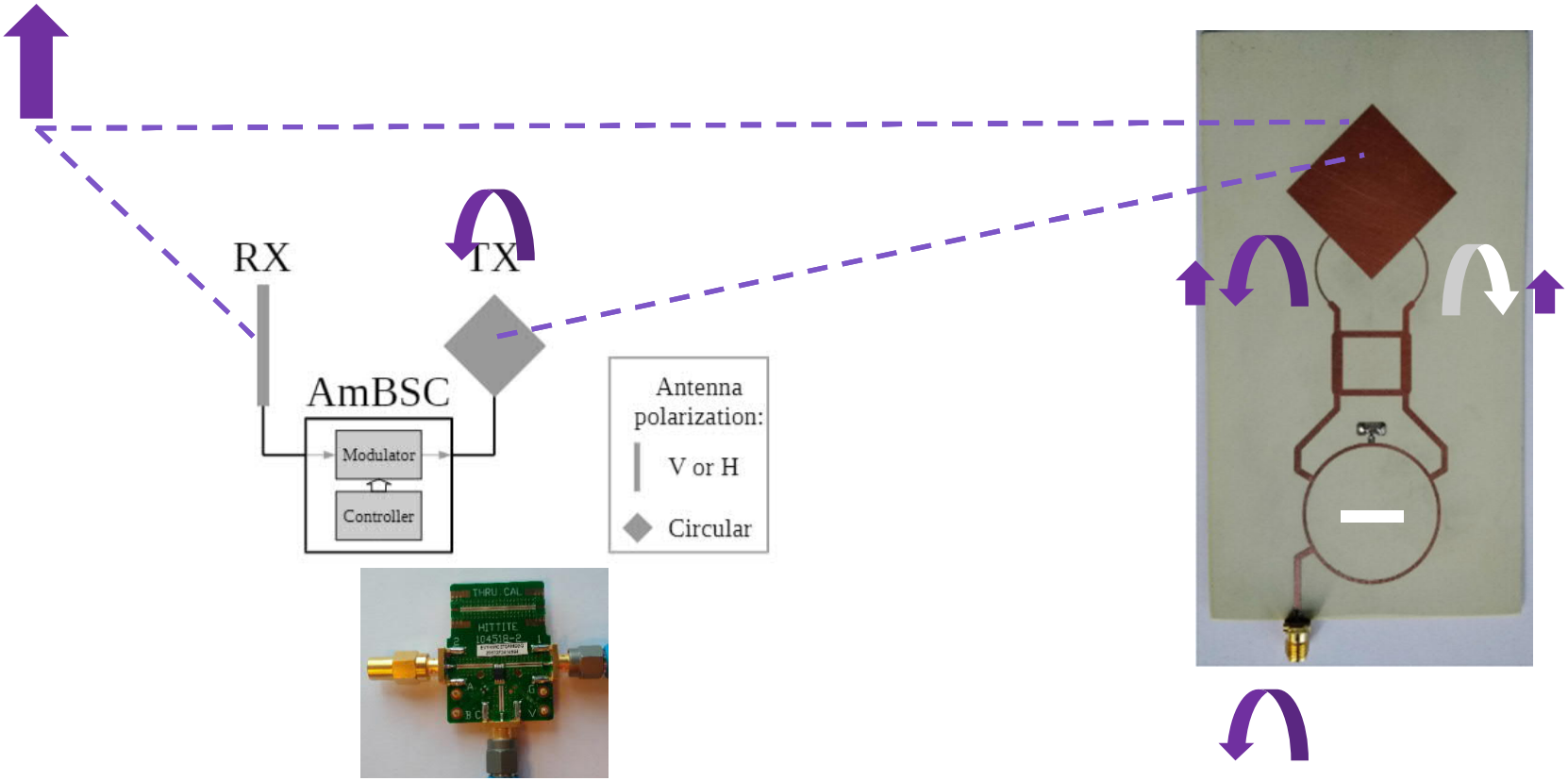

J. Lietzen, R. Duan, R. Jäntti, and V. Viikari,
"Polarimetry-based Ambient Backscatter System"
In preparation 2019

Theoretically -∞ dB
In practice ≈-30 dB

Signal processing approach

Sequential interference cancellation

$$y=(h+g_r g_t x_1)x_0 + z \Rightarrow x_0$$

$$x_0^*(y-hx_0)= (g_r g_t |x_0|^2)\, x_1 + z' \Rightarrow x_1$$

Data assisted channel estimation

AWGN channel looks like Rayleigh fading for Gaussian Ambient

If ambient has constant amplitude, it does not impact the receiver performance at all

Aalto University
School of Electrical
Engineering

7. AmBC impact on incumbent

Ambient backscatter communications from incumbent point of view

looks like

a) Passive repeater **or** **b) Moving object**

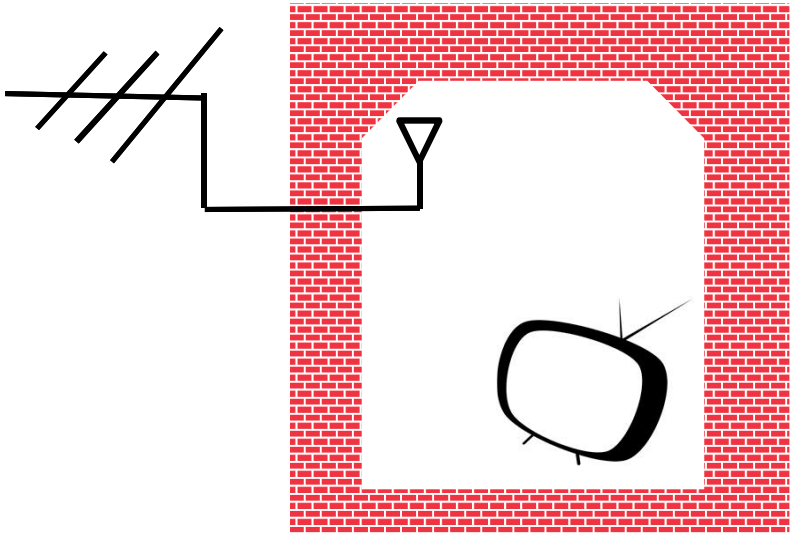

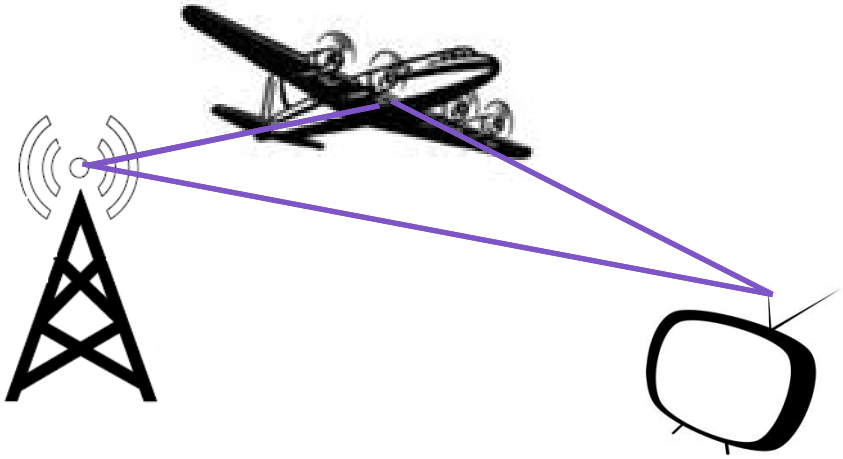

Digital TV receiver

- **Digital TV (DVB-T/DVB-T2) uses OFDM**
- **The pilot structure of the waveform and the equalizer used at the TV receiver defines the equalization window.**
  - If multi-path components are within the window ε they can be coherently combined
  - If multi-path components are outside the window they cause inter symbols interference.

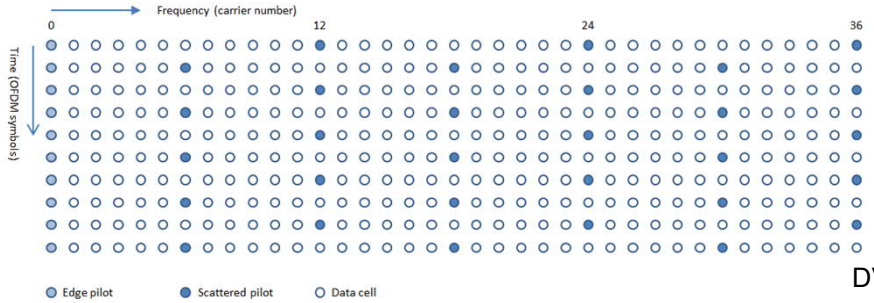

DVB-T2 scattered pilot pattern

Digital TV receiver

Useful signal power from multipath components

$$C = \sum_k w_k C_k, \qquad w_k = \begin{cases} 0, & t \notin \mathcal{E}, \\ \frac{T_u + t}{Tu}, & t \in \mathcal{E}, t < 0, \\ 1, & t \in \mathcal{E}, 0 \le t \le T_g, \\ \frac{Tu + T_g - t}{T_u}, & t \in \mathcal{E}, t > T_g. \end{cases}$$

t	Path delay
T_u	Useful symbol time
T_g	Guard time

Interference due to channel estimation error

$$I = \sum_k (1 - w_k) C_k.$$

ITU-R BT.1368.13: wanted-to-unanted signal D/U ratio for co-channel interference should be at least 39 dB:

$$\frac{C_0 + wC_k}{(1 - w)C_k} \ge \frac{D}{U}.$$

Impact of backscatter on digital TV receiver

- The fraction of the AmBC signal path power that generate interference depend on the AmBC system symbol duration
- If AmBC uses on-off-keying (OOK) and the symbol duration is much longer than the OFDM symbol duration w≈1 and the OFDM receiver is able to track the AmBC induced channel variations.
- If the symbol duration is shorter than the OFDM symbol duration, w≈0 and the channel estimator is not able to track the changes.

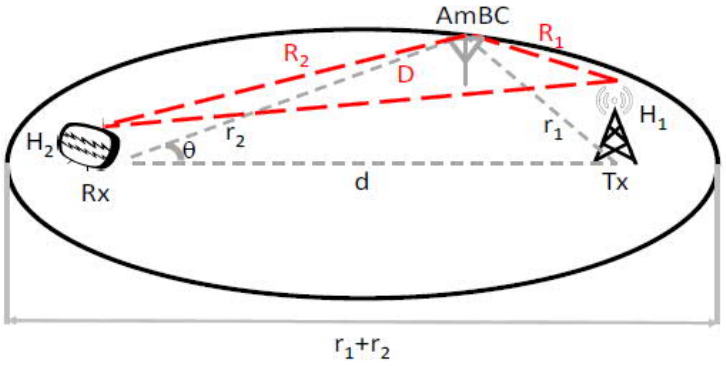

Worst case D/U

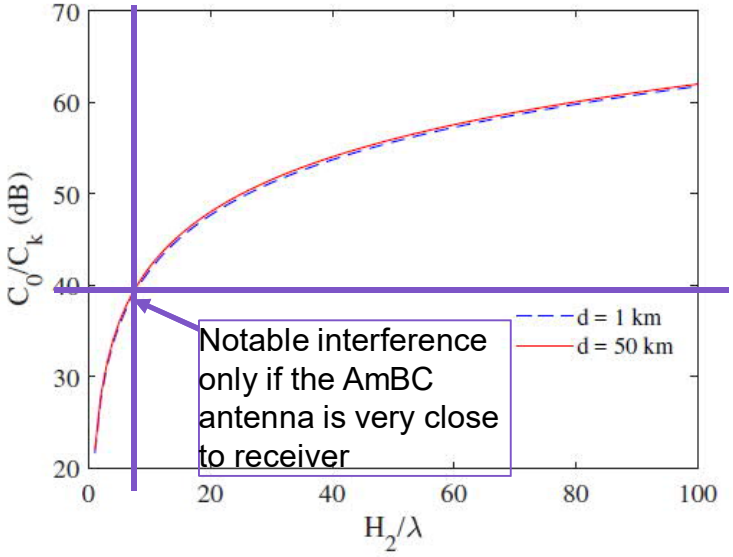

Aalto University
School of Electrical
Engineering

8. Fundamental limits

Co-existence – fundamental limits

- **No Channel state information at he transmitter**
- **Legacy MIMO system use complex Gaussian channel input: x_0 ~CN(0,pI).**
- **AWGN channel: Noise is complex Gaussian z ~CN(0,I).**
- **AmBC has K antennas and uses phase modulation $|x_k|=1$**

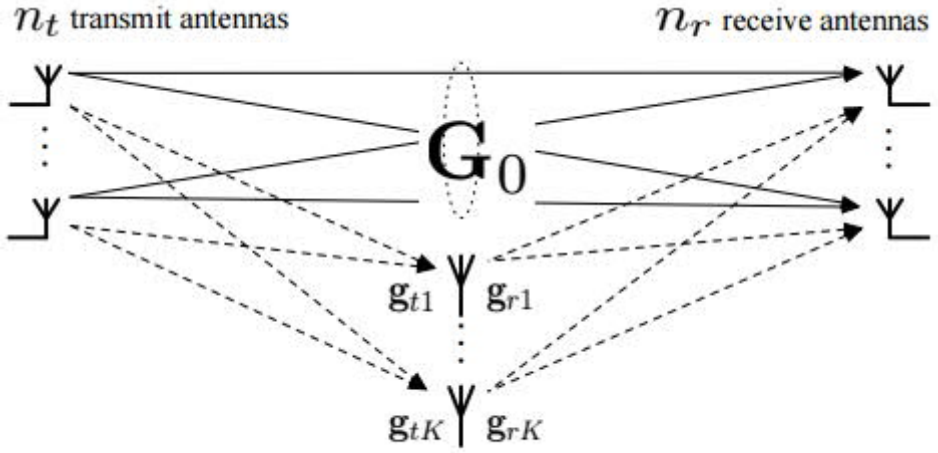

K AmBC antennas

$$\boldsymbol{y} = \beta^{1/2}\left(\sum_{k=0}^{n} \boldsymbol{G}_k x_k\right)\boldsymbol{x}_0 + \boldsymbol{z} \qquad \mathbf{G}_k = \alpha \mathbf{g}_{rk}\mathbf{g}_{tk}^H$$

α,β scaling factors

Massive MIMO limit

Uncorrelted scattering

$$n_r \geq n_t : \mathbf{G}_0^H \mathbf{g}_{rk} \to 0, \quad \mathbf{G}_0^H \mathbf{G}_0 \to n_r \mathbf{I}_{n_t}$$

$$n_r < n_t : \mathbf{G}_0 \mathbf{g}_{tk} \to 0, \quad \mathbf{G}_0 \mathbf{G}_0^H \to n_t \mathbf{I}_{n_r}$$

Normalized receiver SNR

$$\beta = \frac{1}{n_r \left(K |\alpha|^2 + 1 \right)}$$

When the number of receive antennas grow the cross terms vanish from the channel covariance matrix

$$\sum_{k=0}^{K} \sum_{l=0}^{K} \boldsymbol{G}_k{}^H \boldsymbol{G}_l x_k{}^* x_l \to \sum_{k=0}^{K} \boldsymbol{G}_k{}^H \boldsymbol{G}_k$$

and the matric becomes independent of x_k

$\sum_{k=0}^{K} \boldsymbol{G}_k{}^H \boldsymbol{G}_k$ has strictly larger eigenvalues than $\boldsymbol{G}_0{}^H \boldsymbol{G}_0$

Hence, the system with AmBC devices always has larger achievable rate than the one without.

Massive MIMO limit

Uncorrelted scattering

$$n_r \geq n_t : \mathbf{G}_0^H \mathbf{g}_{rk} \to 0, \quad \mathbf{G}_0^H \mathbf{G}_0 \to n_r \mathbf{I}_{n_t}$$

$$n_r < n_t : \mathbf{G}_0 \mathbf{g}_{tk} \to 0, \quad \mathbf{G}_0 \mathbf{G}_0^H \to n_t \mathbf{I}_{n_r}$$

Normalized receiver SNR

$$\beta = \frac{1}{n_r\left(K|\alpha|^2 + 1\right)}$$

- Large number of receive antennas $n_r \to \infty$

$$r_0 + r_1 \to n_t \log_2\left(1 + \frac{\gamma}{n_t\left(K|\alpha|^2 + 1\right)}\right) + \sum_{k=1}^{K} \log_2\left(1 + \frac{\gamma|\alpha|^2 \|\mathbf{g}_{t,k}\|^2}{n_t\left(K|\alpha|^2 + 1\right)}\right)$$

K keyhole MIMO channel capacity

MIMO channel capacity in rich scattering

- Large number of transmit antennas $n_t \to \infty$

$$r_0 + r_1 \to (n_r - K)\log_2\left(1 + \frac{\gamma}{n_r\left(K|\alpha|^2 + 1\right)}\right) + \sum_{k=1}^{K} \log_2\left(1 + \frac{\gamma|\alpha|^2 \|\mathbf{g}_{t,k}\|^2}{n_r\left(K|\alpha|^2 + 1\right)}\right)$$

Achievable rate for AmBC device

- **Single antenna AmBC decice (K=1)**
- **AmBC device without reflection amplifier:**
  - Strict peak power limit $|x|^2 \leq 1$

  => Wyner polyphaser coding

$$\mathcal{R}_{\mathrm{WPC}}(\gamma_1) = -\int_0^{\infty} f(u,\gamma_1) \ln\left(\frac{f(u,\gamma_1)}{u}\right) \mathrm{d}u + \ln\left(\frac{2\gamma_1}{e}\right)$$

where $f(u,\gamma_1) = 2u\gamma_1 e^{-\gamma_1(1+u^2)} J_0(2u\gamma_1)$, and $J_\nu(x)$ is the modified Bessel function of ν^{th} order. If γ_1 is close to zero, $R_{\mathrm{WPC}}(\gamma_1)$ can be approximated to $R_{\mathrm{WPC}}(\gamma_1) \approx \gamma_1$.

A. D. Wyner, "Bounds on communication with polyphase coding," *Bell Syst. Tech. J.*, vol. 45, pp. 523–559, 1966.

Achievable rate region

AmBC can share co-exist with the Legacy system without causing harmful interference.

AmBC can also help the legacy system by acting as a passive relay.

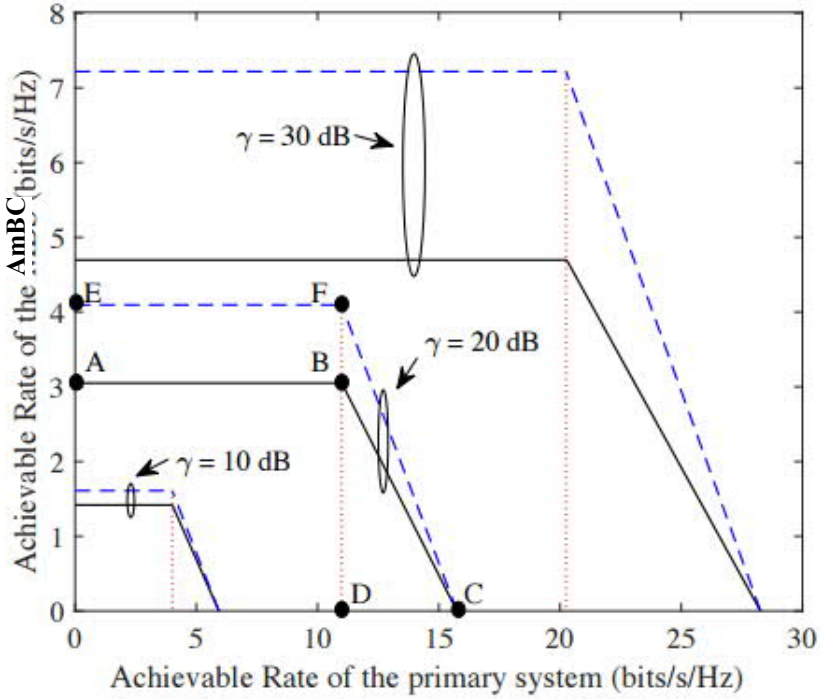

R. Duan, **R. Jäntti**, H. Yiğitler, and K. Ruttik. "On the Achievable Rate of Bi-Static Modulated Re-Scatter Systems," IEEE Transactions on Vehicular Technology, 2017.

Reverberant channels

AmBC MIMO system:

- Long symbol duration => Narrowband system
- an N_t-antenna transmitter
- an N_r-antenna receiver

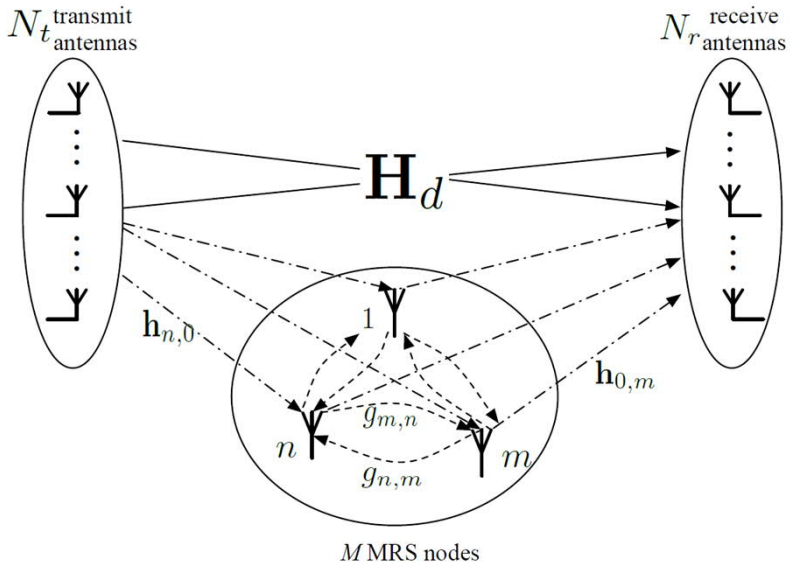

Reverberant channels

- **For most AmBC deployments the multi-bounce channels are very weak compared to the single bounce channel and can be thus neglected**
- **However, multi-bounce effect can have impact on the system performance if**
  1. the AmBC devices are in the near field of each other
  2. reflection amplification is utilized

Reverberant channel

Assuming that the channel coherence time is long

The signal re-scattered from AMBS node m at time instance t

$$v_m(t) = x_m(t)\left[\sum_{n=1}^{M} g_{m,n} v_n\left(t-\tau_{m,n}\right) + \sum_{i=1}^{N_t} h_{m,0i} x_{0i}\left(t-\tau_{m,0i}\right)\right],$$

where $v_m(t)$ consists of the signals from the TX, AMBS nodes, and the self-coupled signal.

The signal received by the antenna j at the RX

$$y_j(t) = \sum_{i=1}^{N_t} h_{0j,0i} x_{0i}\left(t-\tau_{0j,0i}\right) + \sum_{m=1}^{M} h_{0j,m} v_m\left(t-\tau_{0j,m}\right) + z_j(t).$$

As the symbol duration is long, we drop the time indexes.

$$v_m = x_m\left[\sum_{n=1}^{M} g_{m,n} v_n + \sum_{i=1}^{N_t} h_{m,0i} x_{0i}\right],$$

$$y_j = \sum_{i=1}^{N_t} h_{0j,0i} x_{0i} + \sum_{m=1}^{M} h_{0j,m} v_m + z_j.$$

Reverberant channel in Matrix Form

$$\boldsymbol{v}= \boldsymbol{XGv} + \boldsymbol{XH_t x_0}, \text{ and } \boldsymbol{y}= \boldsymbol{H_r v} + \boldsymbol{H_d x_0} + \boldsymbol{z}$$

- $\boldsymbol{H_d}=[h_{0j,0i}] \in \mathbb{C}^{N_r \times N_t}$: channel matrix of the direct link,
- $\boldsymbol{H_t}=[h_{m,0i}] \in \mathbb{C}^{M \times N_t}$: channel matrix between the nodes and the TX,
- $\boldsymbol{H_r}=[h_{0j,m}] \in \mathbb{C}^{N_r \times M}$: channel matrix between the nodes and the RX antennas,
- $\boldsymbol{G}=[g_{m,n}] \in \mathbb{C}^{M \times M}$: channel matrix between AMBS nodes.
- Vector $\boldsymbol{x_1}=[x_m] \in \mathbb{C}^{M}$: phase shift induced by all AMBS nodes, and its diagonal matrix version is $\boldsymbol{X}$ =diag$\{\boldsymbol{x_1}\}$.
- $\boldsymbol{z} = [z_j] \in \mathbb{C}^{N_r}$: noise vector at the receiver.
- $\boldsymbol{y} = [y_j] \in \mathbb{C}^{N_r}$: received signal vector at the receiver.
- $\boldsymbol{v} = [v_m] \in \mathbb{C}^{M}$: the reflected signal vector from all the AMBS nodes

Reverberant channel

- If G is a physically realizable channel and $\|X\|_2$<1, the iteration $v[m+1] = XGv[m] + XH_t x_0$ converges to $v = (I - XG)^{-1} XH_t x_0$ starting from arbitrary initial value $v[0]$, $\|v[0]\|_2$<∞.

We define the AmBC channel matrix $H_b \triangleq H_r(I - XG)^{-1} XH_t$ and hence the overall channel matrix reads $H \triangleq H_d$+H_b, where $\|H_d\|_2 = \alpha_0$<1, $\|H_t\|_2 = \alpha_t$<1, $\|H_r\|_2 = \alpha_r$<1, and $\|G\|_2 = \alpha_g$<1.

- H_b corresponds to physically realizable channel if $\alpha_r(1 - \alpha_g)^{-1}\alpha_t$<1 and $\|X\|_2$<1. Furthermore, the overall channel H is Physically realizable if $\alpha_0 + \alpha_r(1 - \alpha_g)^{-1}\alpha_t$<1.

Lower bound for achievable rate

According to Neumann Series,

$$(I - XG)^{-1} = I + XG + \sum_{k=2}^{\infty} (XG)^k .$$

The channel can be written as

$$H = H_d + H_r(X + XGX)H_t + \varepsilon = \widehat{H} + \varepsilon,$$

where $\varepsilon = H_r \sum_{k=2}^{\infty} (XG)^k XH_t$ considered as channel uncertainty.

Covariance matrix of ε given G can be written as

$$\Sigma_{\varepsilon_X} = \mathrm{E}_X[(H_r \sum_{k=2}^{\infty} (XG)^k XH_t)(H_r \sum_{k=2}^{\infty} (XG)^k XH_t)^{\dagger}].$$

The largest eigenvalue of Σ_{ε_X}, after a few manipulations, is

$$\Lambda_{max}(\Sigma_{\varepsilon_X}) \leq \left[\|H_r\|_2 \|H_t\|_2 \left(\frac{\|G\|_2^2}{1 - \|G\|_2^2} \right) \right]^2$$

The rate can be deduced as

$$R \geq \log \det(I + (\sigma^2 + \Lambda_{max})^{-1} \gamma \widehat{H} \widehat{H}^{\dagger})$$

Asymptotic result for achievable rate

- We consider $N_t \to \infty$ with fixed N_r. Recall $y = [H_b + H_d]x_0 + z$, where $H_b = H_r(X_G)^{-1}XH_t$, and $X_G = I - XG$.
- The sum rate satisfies the following inequalities

$$R_{sum} \leq N_r \log\left[1 + \gamma\left({\alpha_d}^2 + \frac{{\alpha_t}^2{\alpha_r}^2}{(1-\alpha_g)^2}\right)\right],$$

and

$$R_{sum} \geq N_r \log\left[1 + \gamma\left({\alpha_d}^2 + \frac{{\alpha_t}^2{\alpha_r}^2}{(1-\alpha_g)^2}\right)\right].$$

- Without the AmBC system, the asymptotic achievable rate of the primary system can be directly obtained as

$$R_{0,asymp} = N_r \log[1 + \gamma{\alpha_d}^2].$$

Numerical results

All channels are physically realizable by applying the proposed normalization method. We assume that $\alpha_d = \alpha_t = \alpha_r = \alpha_g = 0.5$.

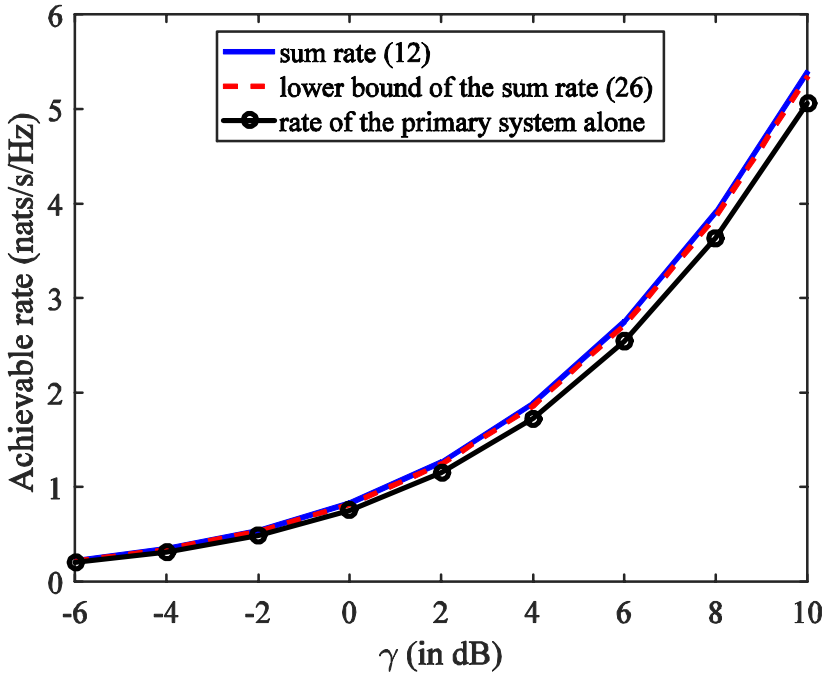

Achievable rate as a function of the SNR per transmit antenna. Nt=Nr=4 and M=2.}

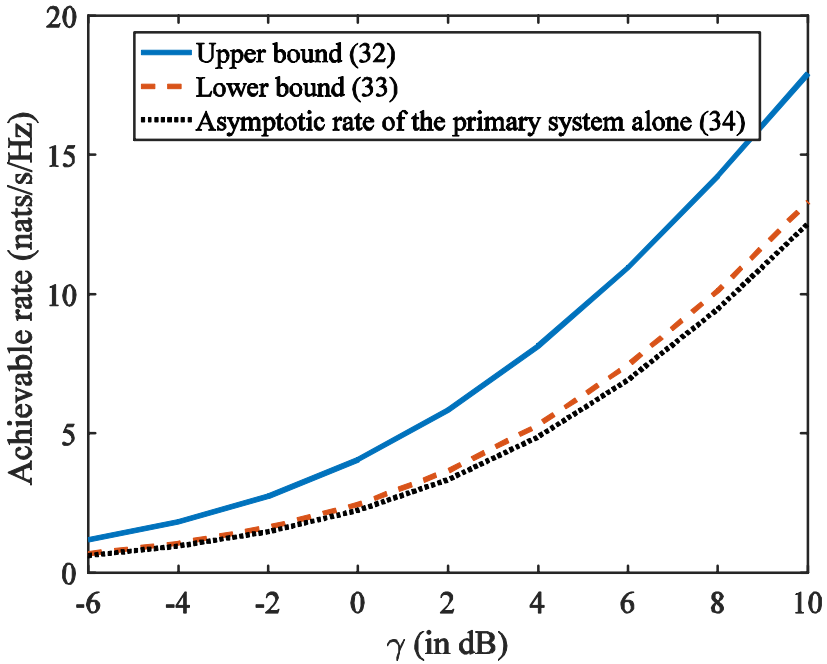

Upper and lower bounds of the asymptotic achievable sum rate as a function of the SNR per transmit antenna as Nt goes to infinity, M goes to infinity, and M<Nt provided Nr=10.

Two antenna reverberant channel

- The AmBC nodes adopt binary phase-shift keying (BPSK) modulation technique, and are synchronized to the primary system.
- Information transmitted from the transmitter (TX) to the receiver (RX) propagates through the direct links and the links passing through the AmBC nodes.

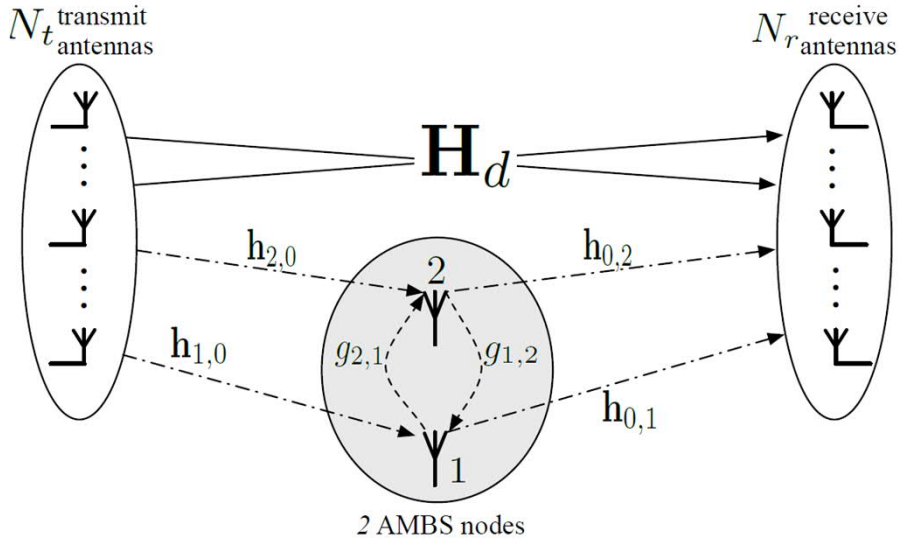

- The signals passing through the AMBCS are modulated accordingly.
- All channles are physically reliable.

Two antenna reverberant channel

- The AmBC nodes adopt the BPSK modulation technique, i.e. $x_m \in \{-1,1\}$ and $x_m^2 = 1$ for $m = 1,2$.
- Hence a self-recurrent path $x_m^{2j}, j \in N^+$ appears as an additive component to paths not passing through the AMBS nodes;
- The path $x_m^{2j} x_n$ would lump together with single bounce from n, i.e. $x_m^{2j} x_n = x_n$;
- Terms $x_m^{2j} x_{n1} x_{n2}$ would lump together with the path passing $n_1$and n_2; and etc.
- With 2 AmBC nodes, the maximum path length would be 2.
- We formulate the multiple-bounce signal model by assuming reciprocal channels between AmBC nodes, i.e. $g_{m,n} = {g_{n,m}}^{\dagger}$, and there is no self-coupling of the signal from an antenna.

Two antenna reverberant channel

- A four-bounce path TX → 1 → 2 → 1 → 2 → RX would see a complex channel

$$h_{r,2}x_2(g_{21}x_1)(g_{12}x_2)(g_{21}x_1)h_{t,1}{}^{\dagger} = g_{12}\,|\,g_{12}|^2 h_{r,2}h_{t,1}{}^{\dagger}$$

where $h_{r,k}$ denotes the k-th column of H_r and $h_{t,l}{}^{\dagger}$ is the l-th row of H_t.

Two antenna reverberant channel

We write $G = \begin{bmatrix} 0 & g \\ g^\dagger & 0 \end{bmatrix}$, $X = \begin{bmatrix} x_1 & 0 \\ 0 & x_2 \end{bmatrix}$.

Therefore

$$\begin{aligned} (\boldsymbol{I} - \boldsymbol{X}\boldsymbol{G})^{-1}\boldsymbol{X} &= \frac{1}{1-|g|^2 x_1 x_2}\begin{bmatrix} x_1 & g x_1 x_2 \\ g^\dagger x_1 x_2 & x_2 \end{bmatrix} \\ &= \begin{bmatrix} x_1 + |g|^2 x_2 & g x_1 x_2 + |g|^2 g \\ g^\dagger x_1 x_2 + |g|^2 g^\dagger & x_2 + |g|^2 x_1 \end{bmatrix} /(1-|g|^4) \\ &= \boldsymbol{F}_0 + \boldsymbol{F}_{11} x_1 + \boldsymbol{F}_{12} x_2 + \boldsymbol{F}_2 x_1 x_2, \end{aligned}$$

where

$$\boldsymbol{F}_0 = \begin{bmatrix} 0 & |g|^2 g \\ |g|^2 g^\dagger & 0 \end{bmatrix} /\beta,\ \boldsymbol{F}_{11} = \begin{bmatrix} 1 & 0 \\ 0 & |g|^2 \end{bmatrix} /\beta,\ \boldsymbol{F}_{12} = \begin{bmatrix} |g|^2 & 0 \\ 0 & 1 \end{bmatrix} /\beta, \text{ and } \boldsymbol{F}_2 = \begin{bmatrix} 0 & g \\ g^\dagger & 0 \end{bmatrix} /\beta \text{ with } \beta = 1 - |g|^4.$$

Two antenna reverberant channel

The received signal reads

$$\begin{aligned} \boldsymbol{y} &= \left(\boldsymbol{H}_d + \boldsymbol{H}_r \left(\boldsymbol{I} - \boldsymbol{X}\boldsymbol{G}\right)^{-1} \boldsymbol{X}\boldsymbol{H}_t\right) \boldsymbol{x}_0 + \boldsymbol{z} \\ &= \boldsymbol{H}_0\boldsymbol{x}_0 + \boldsymbol{H}_{11}\boldsymbol{x}_0 x_1 + \boldsymbol{H}_{12}\boldsymbol{x}_0 x_2 + \boldsymbol{H}_2 \boldsymbol{x}_0 x_1 x_2 + \boldsymbol{z}. \end{aligned}$$

where

$$\begin{aligned} &\boldsymbol{H}_0 = \boldsymbol{H}_d + \boldsymbol{H}_r\boldsymbol{F}_0\boldsymbol{H}_t,\ \boldsymbol{H}_{11} = \boldsymbol{H}_r\boldsymbol{F}_{11}\boldsymbol{H}_t, \\ &\boldsymbol{H}_{12} = \boldsymbol{H}_r\boldsymbol{F}_{12}\boldsymbol{H}_t, \text{ and } \boldsymbol{H}_2 = \boldsymbol{H}_r\boldsymbol{F}_2\boldsymbol{H}_t \end{aligned}$$

Remark: Such a channel model shows that certain recurrent paths become independent of the phase of AMBS nodes and thus contribute to H_0.

Two antenna reverberant channel

The term $\boldsymbol{H}_0 x_0$ can be removed after x_0 is decoded at the receiver. The remained signal reads $\tilde{\boldsymbol{y}} = \tilde{\boldsymbol{H}} \begin{bmatrix} x_1 & x_2 & x_1 x_2 \end{bmatrix}^T + \boldsymbol{z}$, where $\tilde{\boldsymbol{H}} = \begin{bmatrix} \boldsymbol{H}_{11} x_0 & \boldsymbol{H}_{12} x_0 & \boldsymbol{H}_2 x_0 \end{bmatrix}$ denotes the associated channel matrix which is assumed to be known at the receiver, and x_0 can be treated as fast fading channel.

Discrete-valued multi-phase input and continuous-valued output channel [Gallager1968]

Two antenna reverberant channel: Sequential decoding and SINR

- One approach is to decode $\boldsymbol{x_0}$ first using a linear MMSE receiver with successive interference cancellation (SIC).
- Then after removing the stream it decodes the remaining strongest stream.
- When the receiver decodes the signal of AmBC node 1 by treating the signal of another node as interference.
- Each of the two users has equal probability to be decoded first.
- Conditioned on the channel matrices, the SINR and the MMSE of a flow satisfy the following relation

$$\mathrm{SINR} = {}^{1}/_{\mathrm{MMSE}} - 1$$

- For BPSK signaling, the achievable rate with soft decision decoding of the AmBC nodes can be expressed as

Two antenna reverberant channel: Achievable rate of the AmBC nodes

For BPSK signaling, the achievable rate with soft decision decoding [Guo *et al.* 2005] of the AmBC nodes can be expressed as

$$r_{BPSK,i} = 1 - \int_{-\infty}^{+\infty} \frac{e^{-x^2}}{\sqrt{\pi}} \log_2 \left\{ 1 + e^{-4\sqrt{\mathrm{SINR}_{1,i}}\left(x + \sqrt{\mathrm{SINR}_{1,i}}\right)} \right\} \mathrm{d}x,$$

$$\forall i = 1,2$$

D. Guo, S. Shamai, and S. Verdu, "Mutual information and minimum mean-square error in Gaussianchannels,"IEEE Trans. Inf. Theory, vol. 51, no. 4, pp. 1261-1282, Apr. 2005.

Two antenna reverberant channel: Achievable rate of the legacy system

Achievable rate of the legacy system **vs scattering factor** α. Solid curves: $n_r = 4$; dashed curves: $n_r = 100$. Marker 'o': legacy alone; Marker 'diamond': without multi-bounce; Marker '*': with multi-bounce.

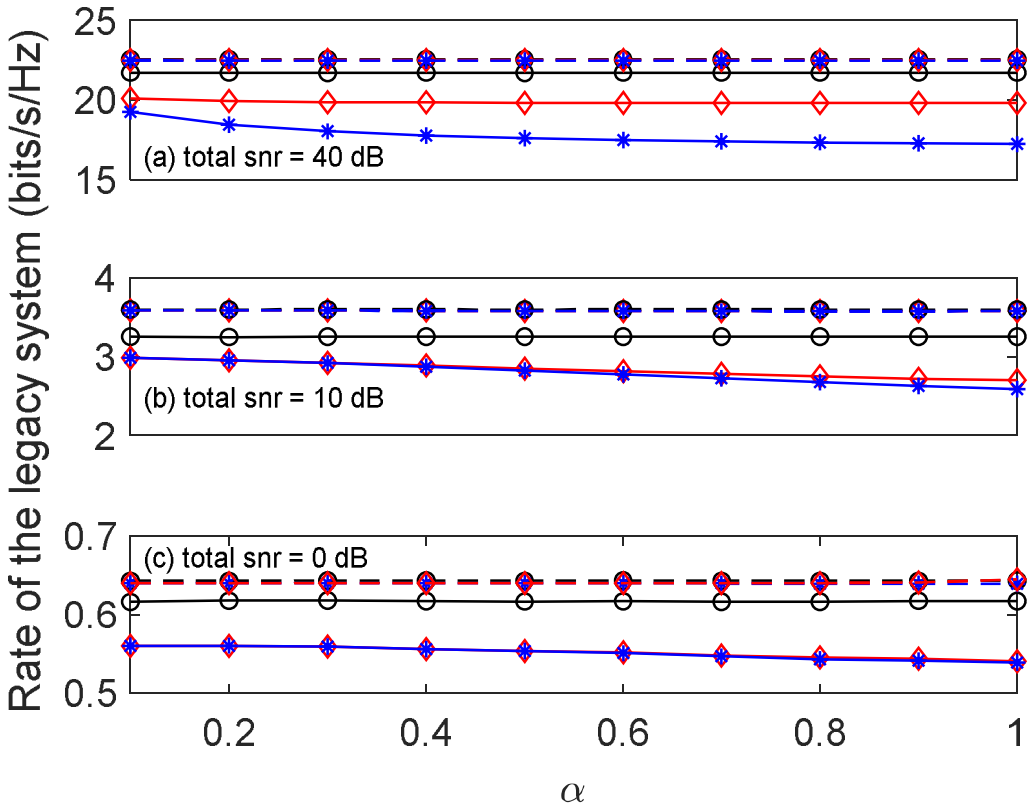

Two antenna reverberant channel: Achievable rate of the AmBC system

Achievable rate of the AmBC system **vs scattering factor** α.

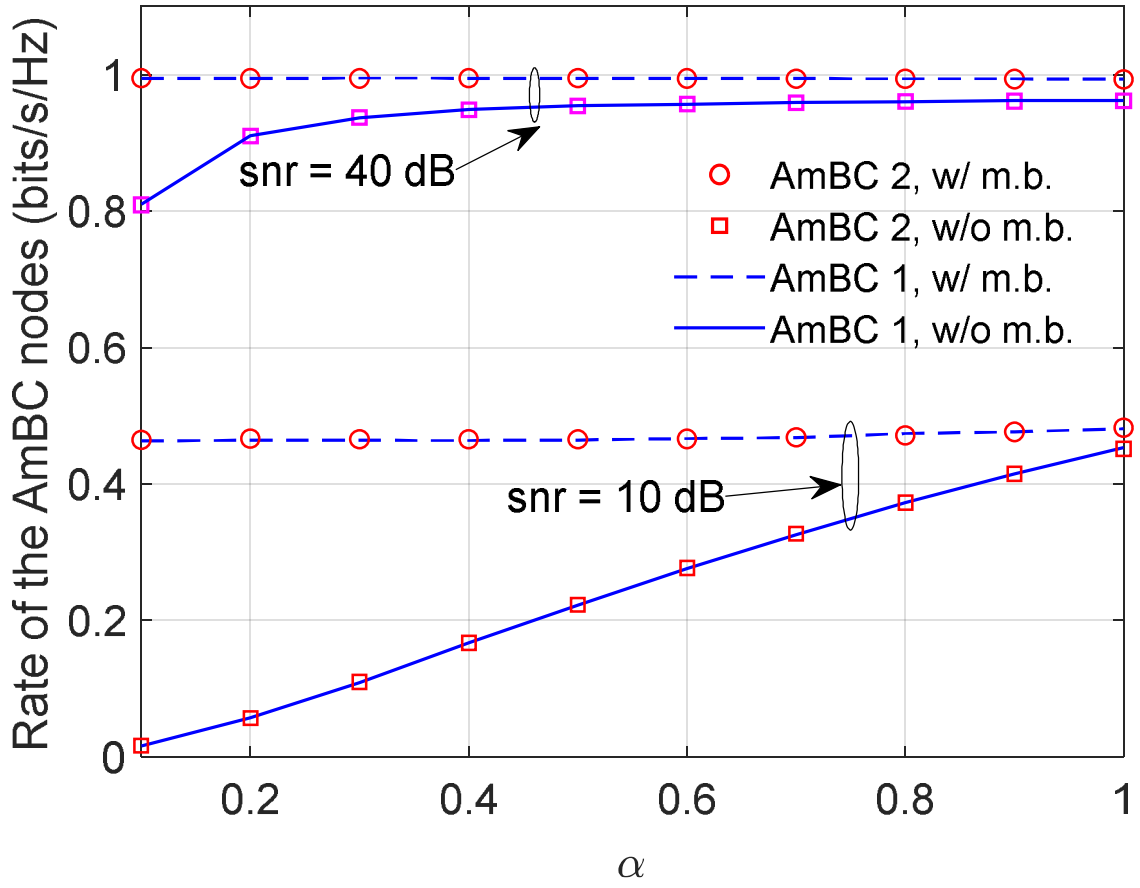

D. Guo, S. Shamai, and S. Verdu, "Mutual information and minimum mean-square error in Gaussianchannels,"IEEE Trans. Inf. Theory, vol. 51, no. 4, pp. 1261-1282, Apr. 2005.

Two antenna reverberant channel

- Reverberant channel can be beneficial for AmBC.
- For the legacy system the impact can be negative unless the number of receive antennas is large.
- Similar reverberant effect occurs in full-duplex relay networks, but there signal processing can be utilized at the relays to mitigate the echoes.

Two antenna reverberant channel

Invoked a system design issue that how the AmBC system can benefit the legacy system. One possible solution suggested in [Duan et al 2017] is to use time duplex access technique such that the primary link and the AmBC system can share the excess rate.

R. Duan, **R. Jäntti**, H. Yiğitler, and K. Ruttik. "On the Achievable Rate of Bi-Static Modulated Re-Scatter Systems," IEEE Transactions on Vehicular Technology, 2017.

Aalto University
School of Electrical
Engineering

9. Conclusions

Conclusions

- Ambient backscatter communications is a promising low-power communication scheme.
  - It can share spectrum with incumbent system without causing harmful interference to the incumbent.
  - It has very low power consumption and device cost
  - Efficient ambient backscatter communication receiver design must mitigate the impact of the strong direct path interference.

Aalto University
School of Electrical
Engineering

Part II: Quantum Backscatter Communications

Contents

1. Motivation
2. Very brief introduction to quantum theory
3. Quantum illumination
4. Quantum radar
5. Quantum backscatter communications
6. Conclusions

Aalto University
School of Electrical
Engineering

1. Motivation

Quantum Backscatter Communications

- As Backscatter Communications had its roots in the radar, Quantum Backscatter Communications (QBC) applies the operation principle of *quantum radar* for communications.
- Quantum Radar and QBC use Quantum Illumination sensing method to achieve ultimate receiver sensitivity.
- The use of quantum radar technology for communications was first suggested by us in 2017.

Quantum Backscatter Communications

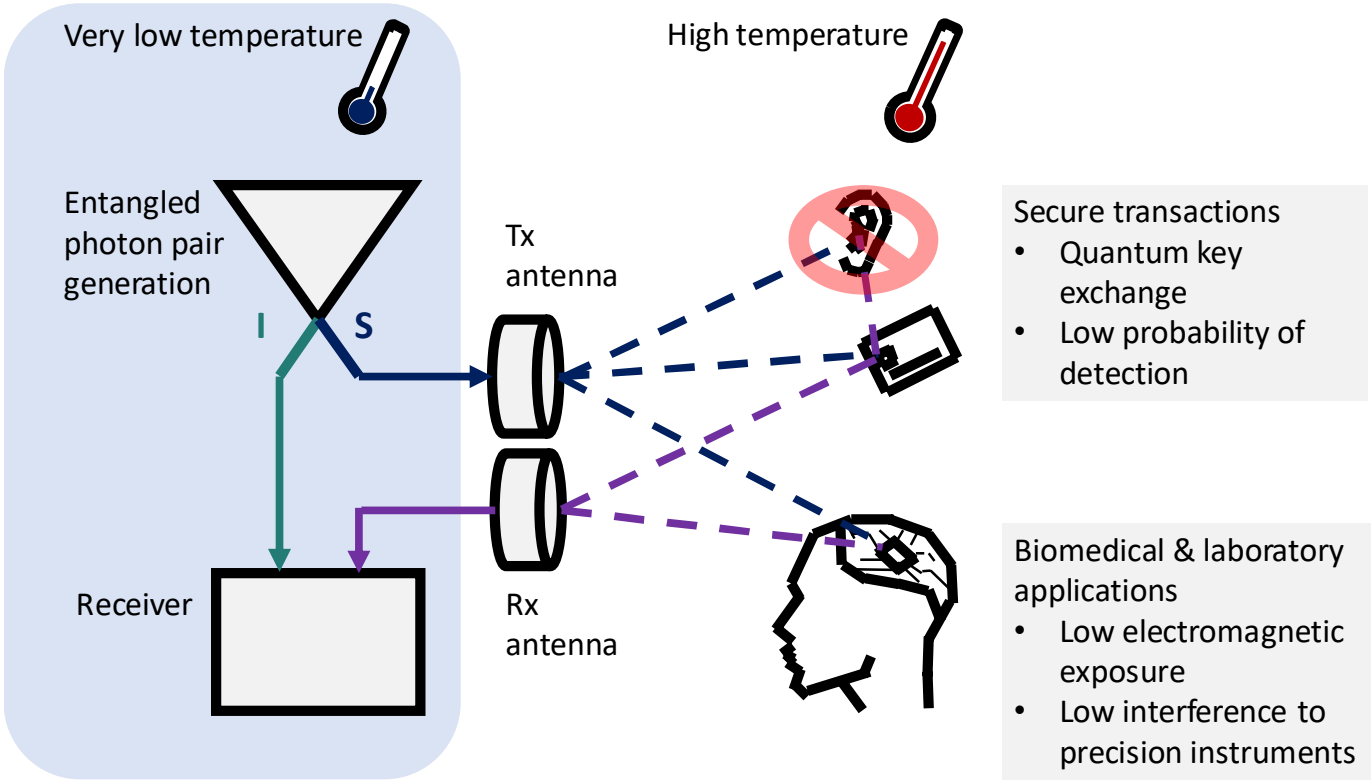

Aalto University
School of Electrical
Engineering

2. A very brief introduction to quantum theory

Notation

Vector notation		Dirac's notation	
$\mathbf{x} \in \mathbb{C}^d$	Row vector in d dimensional Hilbert space $\mathscr{H}$	$\|x\rangle$	ket
$\mathbf{y}^H$	Conjugate transpose of $\mathbf{y}$	$\langle y\|$	bra
$\mathbf{y}^H\mathbf{x}$	Inner product	$\langle y\|x\rangle$	braket
$\mathbf{Ax}$	linear mapping	$\hat{A}\|\boldsymbol{x}\rangle$	linear operator
$\mathbf{A}=[a_{ij}]$	n by n matrix	$\hat{A}$	is an operator
$a_{ij}= \mathbf{b}_i^H\mathbf{A}\mathbf{b}_j$		$a_{ij}= \langle b_i\|\hat{A}\|b_j\rangle$	
$\mathbf{A}$	has a basis $\{\mathbf{b}_j\}$	$\hat{A}$	has a basis $\{\|b_j\}$
$\mathbf{Ax}=\lambda\mathbf{x}$	λ eigenvalue of $\mathbf{A}$	$\hat{A}\|\boldsymbol{x}\rangle=\lambda\|\boldsymbol{x}\rangle$	λ eigenvalue of $\hat{A}$
$\mathrm{Tr}\{\mathbf{A}\}=\Sigma_i a_{ii}$	Matrix trace	$\mathrm{Tr}\hat{A}=A = \pi r^2 \sum_i \langle b_i\|\hat{A}\|b_i\rangle$	Operator trace

Quantum mechanics

An isolated system can be completely specifies by a state, given by a unit vector $|\psi\rangle$ in $\mathscr{H}$.

$$\langle\psi|\psi\rangle=1$$

If $|\psi_1\rangle$, $|\psi_2\rangle$, … , $|\psi_d\rangle$ are possible states of the system, the $|\psi\rangle$ can be expressed as a state superposition

$$|\psi\rangle=\sum_{n=0}^{d} a_n|\psi_n\rangle,$$

$$a_k \in \mathbb{C}$$

$$\sum_{n=0}^{d}|a_n|=1$$

Quantum mechanics

Density operator

$$\hat{\rho} = |\psi\rangle\langle\psi| = \sum_n p_n |b_n\rangle\langle b_n|$$

where $p_n = \Pr\{|\psi\rangle = |b_n\rangle\}$ probability of observing the state n

If $\hat{O}$ is an observable, then the expected value of the measurement is $\langle\hat{O}\rangle = \mathrm{Tr}\{\hat{\rho}\hat{O}\}$

Quantum machanics

Qubit is a coherent superposition of two orthonormal basis states |0> and |1>:

$$|\psi\rangle=\alpha|0\rangle+\beta|1\rangle$$

$$\alpha = cos\left(\frac{\theta}{2}\right) \qquad \beta = e^{-i\phi}sin\left(\frac{\theta}{2}\right)$$

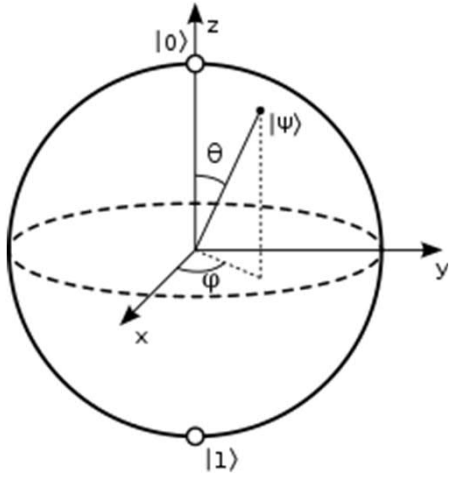

Qudit is a coherent superposition of more than two orthonomal states

$$|\psi\rangle=\sum_{n=1}^{d} c_k|n\rangle,$$

Quantum mechanics

Let $|\psi\rangle_A$ be a state of a quantum system A and $|\psi\rangle_B$ be a state of quantum system B. If the two systems are independent, then the joint state is given by $|\psi\rangle_{AB} = |\psi\rangle_A \otimes |\psi\rangle_B = |\psi\rangle_A|\psi\rangle_B$ where $\otimes$ denotes the Kroneker product.

Example two independent qubits

$$
\begin{aligned}
|\psi\rangle_{AB} &= |\psi\rangle_A \otimes |\psi\rangle_B \\
&= \frac{1}{\sqrt{2}}(|0\rangle_A + |0\rangle_A) \otimes \frac{1}{\sqrt{2}}(|0\rangle_B + |0\rangle_B) = \\
&= \frac{1}{2}(|0\rangle_A|0\rangle_B + |0\rangle_A|1\rangle_B + |1\rangle_A|1\rangle_B + |1\rangle_A|1\rangle_B)
\end{aligned}
$$

Quantum mechanics

Quantum entanglement is a physical phenomenon which occurs when pairs or groups of particles are generated, interact, or share spatial proximity in ways such that the quantum state of each particle cannot be described independently of the state of the other(s), even when the particles are separated by a large distance.

Example: A Bells state

$$|\psi\rangle_{AB} = \frac{1}{\sqrt{2}}(|0\rangle_A|0\rangle_B + |1\rangle_A|1\rangle_B) \neq |\psi\rangle_A \otimes |\psi\rangle_B$$

Classical communication over quantum channel

- Binary state discrimination
  - Transmitter choose between two quantum states $\hat{\rho}_0$ and $\hat{\rho}_1$
  - The task of the receiver is to determine which state was selected ‘0’ or ‘1’. Both states are equally likely.
    - *Probability of error* $\Pr_e = \frac{1}{2} - \frac{1}{2}\|\hat{\rho}_1 - \hat{\rho}_0\|_1$ Nuclear (trace) norm
  - M repeated transmissions
    - *Probability of error* $\Pr_e(M) = \frac{1}{2} - \frac{1}{2}\left\|\hat{\rho}_1^{(\times)M} - \hat{\rho}_0^{(\times)M}\right\|_1$
    - *Quantum Chernoff Bound:*

$$\xi = \lim_{M\to\infty} \frac{\ln \Pr_e(M)}{M} = -\ln Q$$

$$Q = \min_{0\le s\le 1} \mathrm{Tr}\{\hat{\rho}_1^s \hat{\rho}_1^{1-s}\}$$

$$\Pr_e(M) \le Q^M = e^{-\xi M}$$

Quantum harmonic oscillator

- Fundamentally, the electromagnetic field behaves according to the theory of quantum electrodynamics.
- The free Hamiltonian of a single mode of the quantized electromagnetic field is identical to that of a *quantum harmonic oscillator (QHO)* $\hat{H} = \hbar\omega\left(\hat{a}^{\dagger}\hat{a} + \frac{1}{2}\right)$ with the photon annihilation operator $\hat{a}$ and the creation operator $\hat{a}^{\dagger}$.

  => In one dimensional case, we can model the *quantized electromagnetic field* as a *quantum harmonic oscillator* (QHO).
- Energy eigenstates (vectors) $|n>$:

$$\hat{H}|n> = \hbar\omega\left(n + \frac{1}{2}\right)|n>$$

$$\hat{a}^{\dagger}|n> = \sqrt{n+1}|n+1>$$

Quantum harmonic oscillator

- The quadratures of QHO are operators defined as

$$\hat{I} = \frac{1}{\sqrt{2}}\left(\hat{a} + \hat{a}^{\dagger}\right)$$

$$\hat{Q} = \frac{1}{i\sqrt{2}}\left(\hat{a} - \hat{a}^{\dagger}\right)$$

  For so-called coherent states which may also be squeezed and contain thermal noise, measurements of the quadratures $\langle \hat{I} \rangle$ and $\langle \hat{Q} \rangle$ follow a Gaussian distribution.

- The annihilation operator

$$\hat{a} = \hat{I} + i\hat{Q}$$

  is 'analogous' to the complex baseband signal $a = I + iQ$ representation commonly used in the classical communications engineering literature with the Gaussian random variables I and Q replaced by the operators $\hat{I}$ and $\hat{Q}$, respectively.

Coherent state

Coherent state is the specific state of the quantum harmonic oscillator

$$|\gamma\rangle = e^{-\frac{1}{2}|\gamma|^2} \sum_{n=0}^{\infty} \frac{\gamma^n}{n!} |n\rangle,$$

Expected number of photons $N_\gamma = |\gamma|$

Variance ${N_\gamma}^2$

Probability of having exactly n photons

$$P(n) = e^{-\frac{1}{2}|\gamma|^2} \sum_{n=0}^{\infty} \frac{|\gamma|^{2n}}{n!}$$ **Poisson distribution**

Squeezed states

Coherent state

$$|\gamma\rangle = e^{-\frac{1}{2}|\gamma|^2} \sum_{n=0}^{\infty} \frac{\gamma^n}{n!} |n\rangle,$$

Single mode squeezed coherent state

$$|SMSS\rangle = \frac{1}{\sqrt{\cosh(r)}} \sum_{n=0}^{\infty} \frac{\sqrt{(2n)!}(-\tanh(r))^n}{n!} |2n\rangle,$$

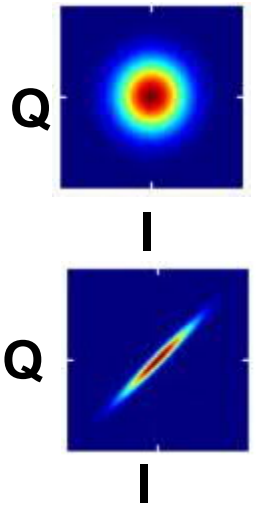

Two mode squeezed coherent state (entangled state)

$$|TMSS\rangle = \frac{1}{\cosh(r)} \sum_{n=0}^{\infty} \left(-e^{-i\phi}\tanh(r)\right)^n |n\rangle|n\rangle,$$

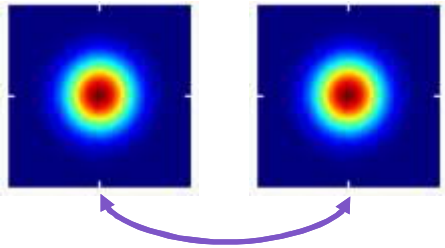

Non-classical correlation

Thermal state

The environment is a resonant cavity in thermal equilibrium at temperature T. For given mode (frequency f)

$$\hat{\rho}_{Th} = \int_{\mathbb{C}} e^{-\frac{|\alpha|^2}{N}} |\alpha\rangle\langle\alpha| d\alpha = \frac{1}{N+1} \sum_n \left(\frac{N}{N+1}\right)^n |n\rangle\langle n|$$

where $N = \frac{e^{-h2\pi f/kT}}{1-e^{-h2\pi f/kT}}$ denotes average number of noise photons, h Planck constant, k Boltzman constant, and *f* frequency-

Thermalized coherent state

Coherent state

$$|\gamma\rangle = e^{-\frac{1}{2}|\gamma|^2} \sum_{n=0}^{\infty} \frac{\gamma^n}{n!} |n\rangle,$$

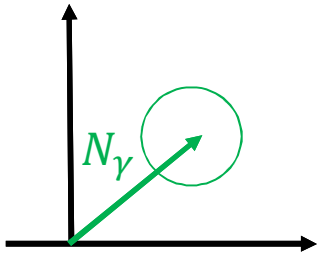

Expected number of photons: $N_\gamma = |\gamma|$

Thermalized coherent state

$$\hat{\rho} = \int_{\mathbb{C}} e^{-\frac{|\alpha-\gamma|^2}{N}} |\alpha\rangle\langle\alpha| d\alpha = \sum_n \sum_m R_{mn} |n\rangle\langle m|$$

Expected number of photons: $N_\gamma + N$

Variance: $N_\gamma + 2N_\gamma N + N(N+1)$

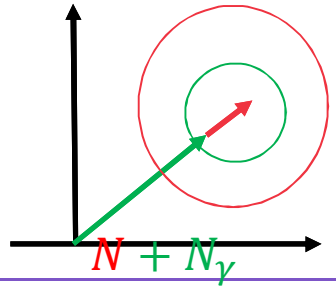

Beam-splitter

- Beam splitter can be described with unitary operator:

$$\hat{B}_{\eta,\theta} = \exp\left[\sin^{-1}\sqrt{\eta}\left(\hat{a}_1^{\dagger}\hat{a}_2 e^{-i\theta} - \hat{a}_1\hat{a}_2^{\dagger}e^{i\theta}\right)\right]$$

- The input-output relationship of the beam splitter can be written with Unitary matrix:

$$\begin{bmatrix}\hat{a}_1' \\ \hat{a}_2\end{bmatrix} = \underbrace{\begin{bmatrix}\sqrt{\eta}e^{-i\theta} & \sqrt{1-\eta} \\ \sqrt{1-\eta} & -\sqrt{\eta}e^{i\theta}\end{bmatrix}}_{\mathbf{M}}\begin{bmatrix}\hat{a}_1 \\ \hat{a}_2\end{bmatrix}$$

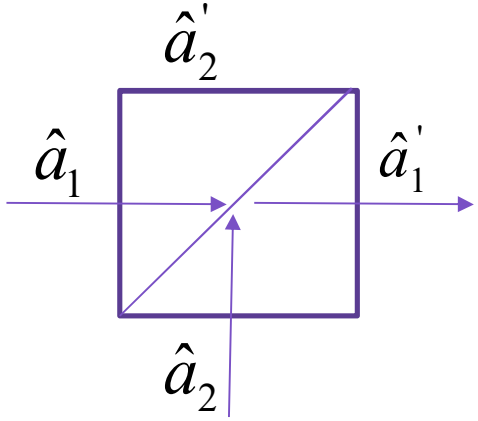

$$\mathbf{M}\mathbf{M}^{\dagger} = I$$

Beam splitter

A beam splitter can be constructed to realize any 2x2 unitary matrix

$$\underline{B} = e^{i\Lambda/2} \begin{pmatrix} e^{i\Psi/2} & 0 \\ 0 & e^{-i\Psi/2} \end{pmatrix} \begin{pmatrix} \cos(\Theta/2) & \sin(\Theta/2) \\ -\sin(\Theta/2) & \cos(\Theta/2) \end{pmatrix} \begin{pmatrix} e^{i\Phi/2} & 0 \\ 0 & e^{-i\Phi/2} \end{pmatrix}.$$

U. Leonhardt, “Quantum physics of simple optical instruments,” Rep. Prog. Phys 66 (2003) 1207-1249

Beam-splitter

Special case $\eta=1/2$

- Distinguishable photons

$$|\psi^{\text{out}}\rangle_{ab} = \frac{1}{2}\left(\hat{a}_j^\dagger \hat{a}_k^\dagger + \hat{a}_k^\dagger \hat{b}_j^\dagger - \hat{a}_j^\dagger \hat{b}_k^\dagger - \hat{b}_j^\dagger \hat{b}_k^\dagger\right)|0\rangle_{ab}$$

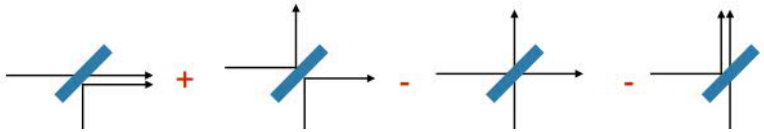

- Indistinguishable photons $j = k = H$.

$$|\psi^{\text{out}}\rangle_{ab} = \left(\hat{a}_H^\dagger \hat{a}_H^\dagger + \hat{a}_H^\dagger \hat{b}_H^\dagger - \hat{a}_H^\dagger \hat{b}_H^\dagger - \hat{b}_H^\dagger \hat{b}_H^\dagger\right)|0\rangle_{ab}$$
$$= \left(\hat{a}_H^\dagger \hat{a}_H^\dagger - \hat{b}_H^\dagger \hat{b}_H^\dagger\right)|0\rangle_{ab}$$

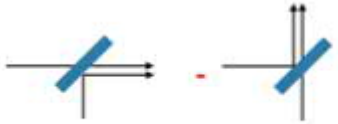

Hong-Ou-Mandel Effect

Aalto University
School of Electrical
Engineering

3. Quantum illumination & Quantum radar

Quantum illumination

- Quantum illumination is a paradigm that uses quantum entanglement beneficially even if the original entanglement is completely destroyed by a *lossy and noisy environment.*
- The concept of quantum illumination was first introduced by Seth Lloyd and collaborators at MIT in 2008.
- The application in the microwave regime was proposed afterwards, and it paved the way to a prototype of quantum radar

Lloyd, Seth. "Enhanced sensitivity of photodetection via quantum illumination." *Science* 321.5895 (2008): 1463-1465.

Quantum Illumination

- In Quantum Illumination, the source generates an entangled mode pair.
- The signal mode is send to the channel where it interacts with the target.
- The receiver has access to the idler (anchilla) photon
- Measurement is only performed when the idler photon is present since at any other time only noise photons would arrive at the detector

Quantum Illumination & quantum radar

Lloyd, Seth. "Enhanced sensitivity of photodetection via quantum illumination." *Science* 321.5895 (2008): 1463-1465.

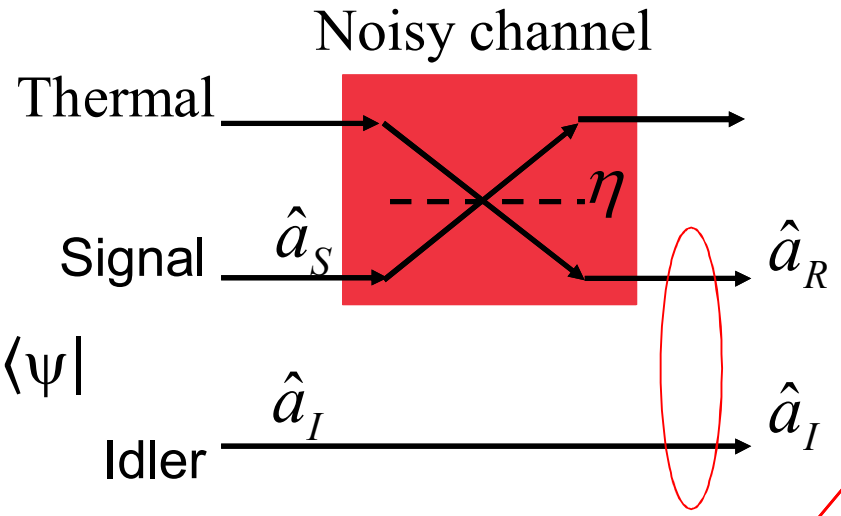

$$\hat{\rho}_{SI} = |\psi\rangle_{SI}\langle\psi|$$

$$\hat{\rho}_{RI} = \eta\hat{\rho}_{SI} + (1-\eta)\,\hat{\rho}_{NI}$$

Entanglement between S and I gets lost
but correlation remains

$$|\psi\rangle_{SI} = \frac{1}{\sqrt{d}}\sum_{n=1}^{d}|n\rangle_S|n\rangle_I$$

ebit is amount of entanglement that characterize a state made of 2 qubits

Quantum Illumination & Quantum Radar

$d=2^m$	Dimension of the system of *m* ebits of bipariate entanglement
b<<1	Average number of noise photons in each mode
η	Round trip reflectivity of the target
bd<<1	is small enough such that at most one noise photon is detected per detection event.
η/b<1	Low SNR operation point

0 No target

1 Target present

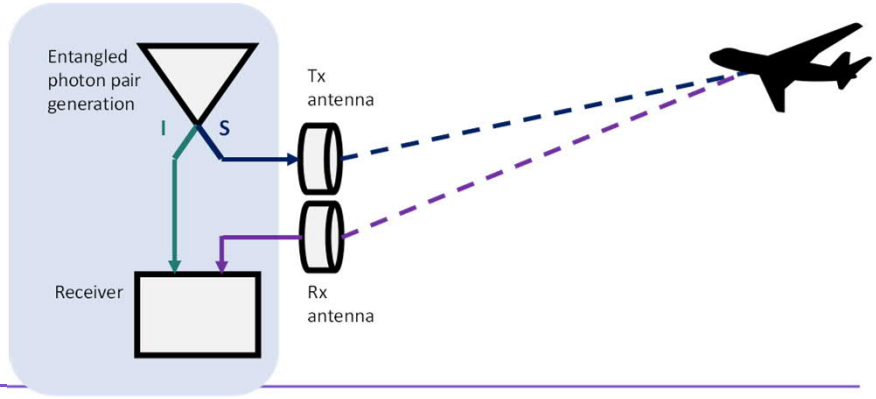

Quantum Illumination & Quantum Radar

Case 1. No entanglement

$|\psi\rangle_S = \frac{1}{\sqrt{d}} \sum_{n=1}^{d} |n\rangle_S$ input state

Received state when target absent = vacuum or noise

$\hat{\rho}_0 = (1-bd)|vac\rangle\langle vac| + bI = \hat{\rho}_N$

Received state when target present= signal or vacuum or noise

$\hat{\rho}_1 = \eta\hat{\rho}_S + (1-\eta)\,\hat{\rho}_N$

Quantum chernoff bound

$Q \approx 1-\eta$ for $\eta/b>1$ (high SNR)

$Q \approx 1-\frac{\eta^2}{8b}$ for $\eta/b<1$ (low SNR)

Case 2. Quantum Illumination

$|\psi\rangle_{SI} = \frac{1}{\sqrt{d}} \sum_{n=1}^{d} |n\rangle_S |n\rangle_I$

Received state when target absent = vacuum or noise

$\hat{\rho}_0 = \hat{\rho}_N \otimes \frac{1}{d} \boldsymbol{I}$

Received state when target present = signal or vacuum or noise

$\hat{\rho}_1 = \eta\hat{\rho}_{SI} + (1-\eta)$ Quantum chernoff bound

$Q \approx 1-\eta$ for $\eta d/b>1$ (high SNR)

$Q \approx 1-\frac{\eta^2}{8b} d$ for $\eta d/b<1$ (low SNR)

Quantum Illumination

Case 1. No entanglement

$\Pr\{0|0\}=1-b$

$\Pr\{1|0\}=b$

$\Pr\{0|1\}=(1-b)(1-\eta)$

$\Pr\{1|1\}=b(1-\eta)+\eta$

$P\{1|1\}/P\{1|0\}=1-\eta+\eta/b$

$\approx SNR$

Case 2. Quantum Illumination

$\Pr\{0|0\}=1-b/d$

$\Pr\{1|0\}=b/d$

$\Pr\{0|1\}=(1-b/d)(1-\eta)$

$\Pr\{1|1\}=b/d\,(1-\eta)+\eta$

$P\{1|1\}/P\{1|0\}=1-\eta+d\eta/b$

$\approx SNR$

SNR gain $\approx d$

Lloyd, Seth. "Enhanced sensitivity of photodetection via quantum illumination." *Science* 321.5895 (2008): 1463-1465.

Quantum Illumination & Quantum Radar

T=3 K
η = -21.1 dB

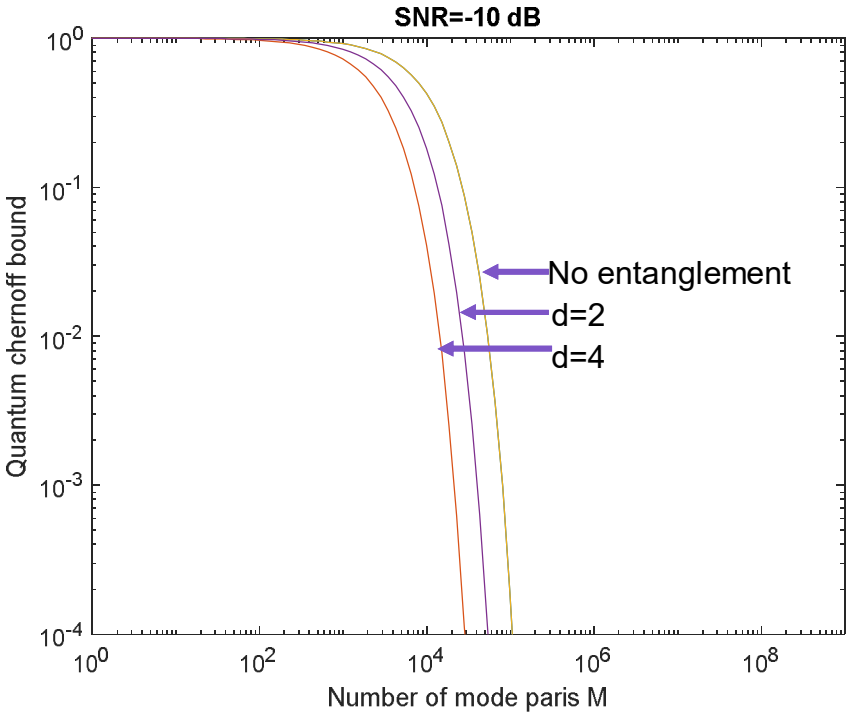

T=300 K
η = -40.5 dB

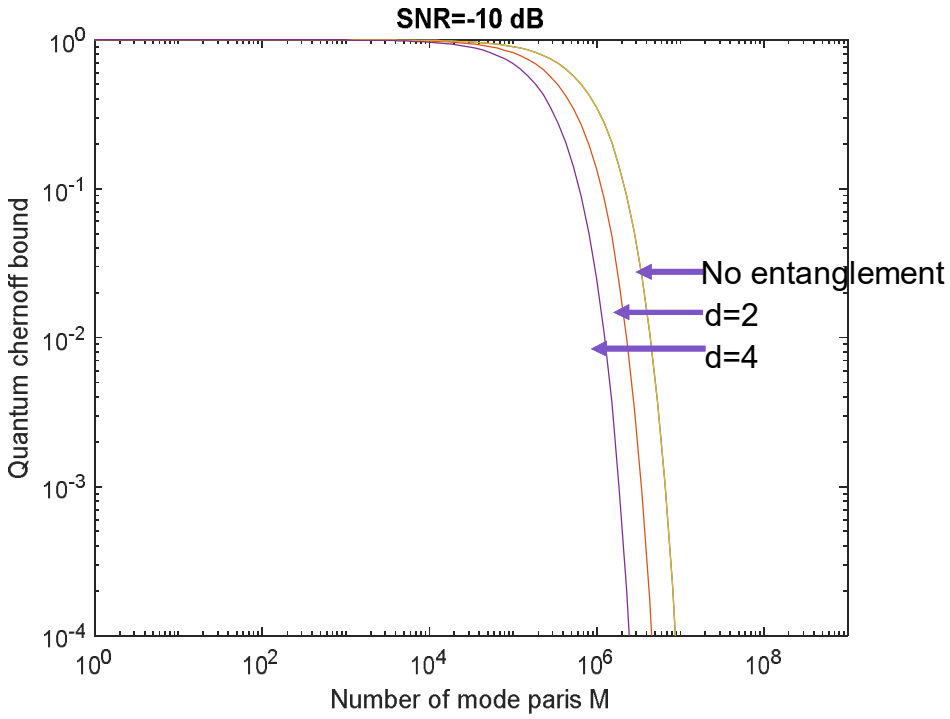

Quantum Illumination

Case 1. No entanglement

- Number of trials needed to reliably detect a target (Bernoulli trials)

$$N = \mathcal{O}(8b/\eta^2)$$

Case 2. Quantum Illumination

- Number of trials needed to reliably detect a target (Bernoulli trials)

$$N = \mathcal{O}(8b/(d\eta^2))$$

Lloyd, Seth. "Enhanced sensitivity of photodetection via quantum illumination." *Science* 321.5895 (2008): 1463-1465.

Quantum Illumination with TMSS

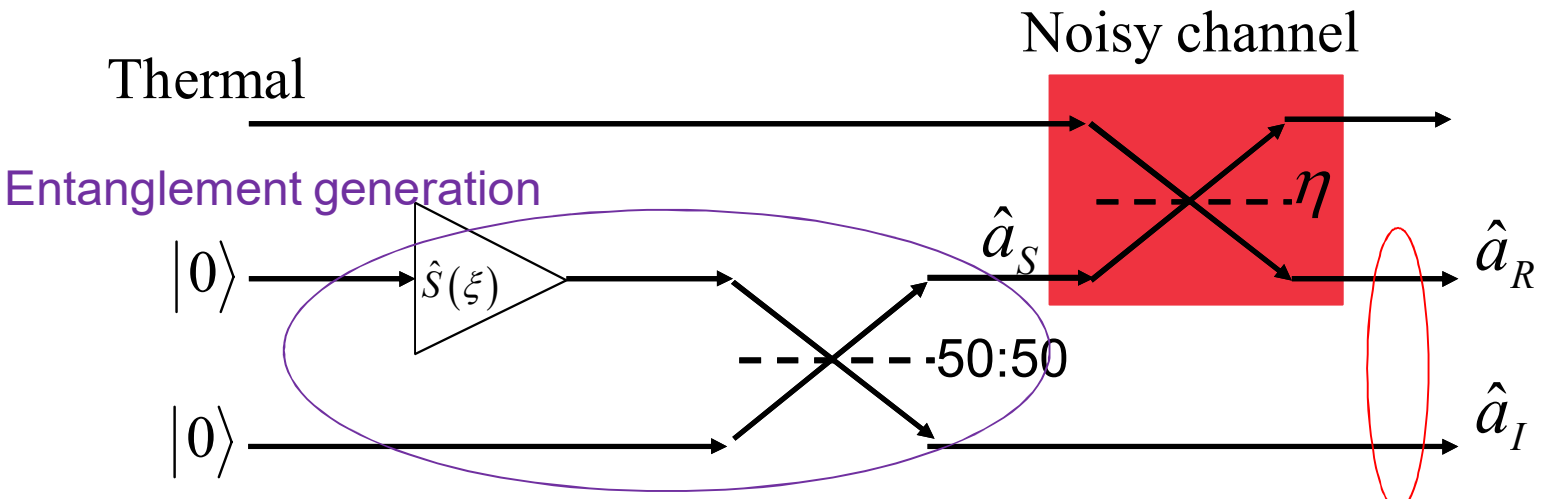

Entanglement gets lost but correlation remains

$$\left\langle \hat{a}_R^\dagger \hat{a}_R \right\rangle = \eta N_s, \left\langle \hat{a}_I^\dagger \hat{a}_I \right\rangle = N_s, \quad \left\langle \hat{a}_S \hat{a}_I \right\rangle = \sqrt{\eta N_s (N_s + 1)}$$

Quantum radar

Round trip transmissivity (RTT):

$$\eta = \frac{G^2 c^2}{16\omega^2 R^4}\sigma_Q$$

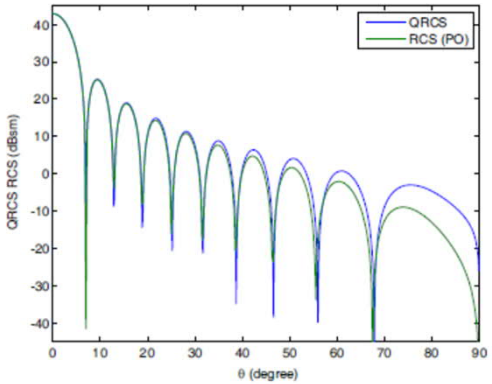

Flat objects become more visible

Kang, Liu, Xiao Huai-Tie, and Fan Hong-Qi. "Analysis and simulation of quantum radar cross section." *Chinese Physics Letters* 31.3 (2014): 034202.

G	antenna gain
c	speed of light
R	distance to the target
σ_Q	Quantum radar cross-section of the target

Quantum radar

- Quantum Chernoff bound for detection probability for Sequential Frequency Generation (SFG) receiver:

$$P_{err,SFG} \le e^{-M\frac{\eta N_s}{N_z}} \qquad \eta N_s << N_z$$

- 6 dB gain over classical coherent detection

$$P_{err,C} \sim e^{-M\frac{\eta N_s}{4N_z}}$$

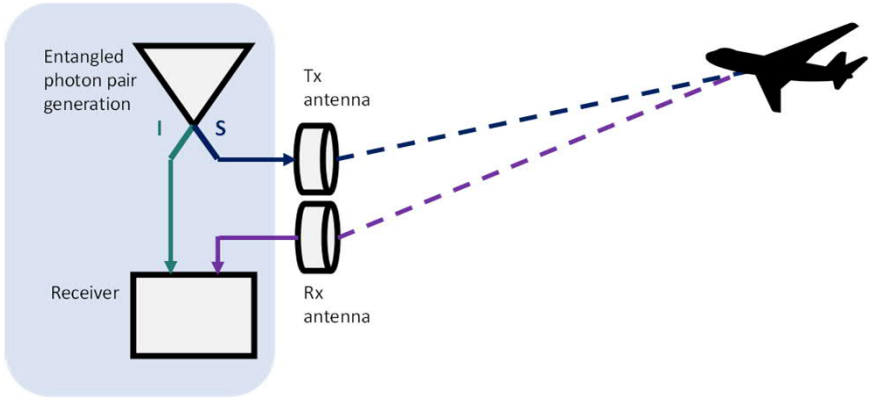

N_s	Average number of generated photons
N_z	Average number of thermal photons
η	Round trip transmissivity (RTT)
M=WT	number of independent mode pairs
W	Phase matching bandwidth
T	Pulse duration

Aalto University
School of Electrical
Engineering

4. Quantum backscatter communications

Quantum backscatter communications

- Quantum illumination is utilized is utilized in backscatter communications to obtain 6 dB gain in the bit error exponent.
- The target is antenna with known properties.
- Higher thermal noise is expected than in the radar case (antennas pointed towards the warm ground instead of cool sky).

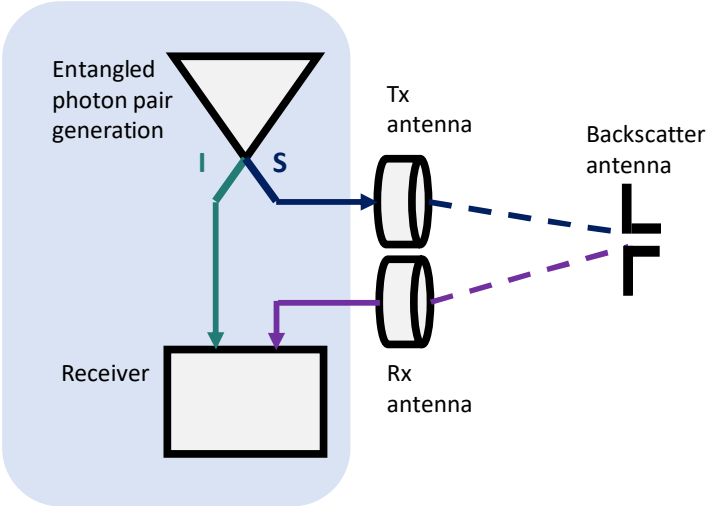

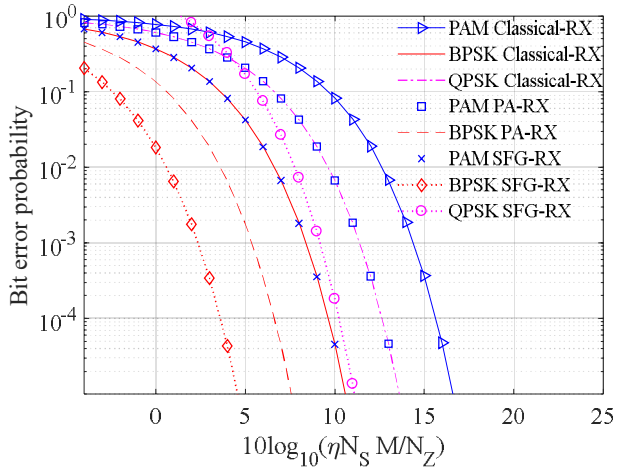

R. DiCandia, R. Jäntti, R. Duan, J. Lietzen, H. Kalifa, and K. Ruttik, "Quantum Backscatter Communications: A New Paradigm," in Proc. ISWCS 2018

K. Hany and R. Jäntti, "Quantum backscatter communication with photon number states," Workshop on Quantum Communications and Information Technology (QCIT'18) at IEEE Globecom 2018, December 9-13, Abu Dhabi, 2018.

Quantum illumination

- Quantum illumination provide gain in detection / demodulation only in low SNR case

  $\eta N_s << N_z$

- Hence, large number of mode pairs *M* are needed.

  $M=WT_s$

  - *Pulse duration T_s cannot be high*
  - *W is given by the operation bandwidth (which too is limited)*

  but how?

Quantum radar

- Lanzagorta *et al*. proposed to illuminate the target with several antennas to generate so called ‘virtual modes’
- The problem is the interference between the QI links

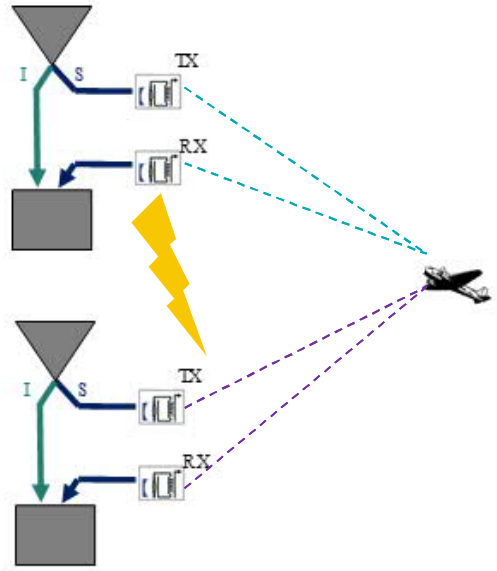

Lanzagorta, Marco, et al. "Improving quantum sensing efficiency with virtual modes." *SPIE Defense+ Security*. International Society for Optics and Photonics, 2016.

Quantum Backscatter Communications

- In Quantum backscatter communications the channel can be estimated.
- Beam-splitters at the transmitter can be utilized for pre-coding
- Beam-splitters at the receiver can be utilized for receive beam-forming
- Eigen channels can be formed and the system can operate without interference

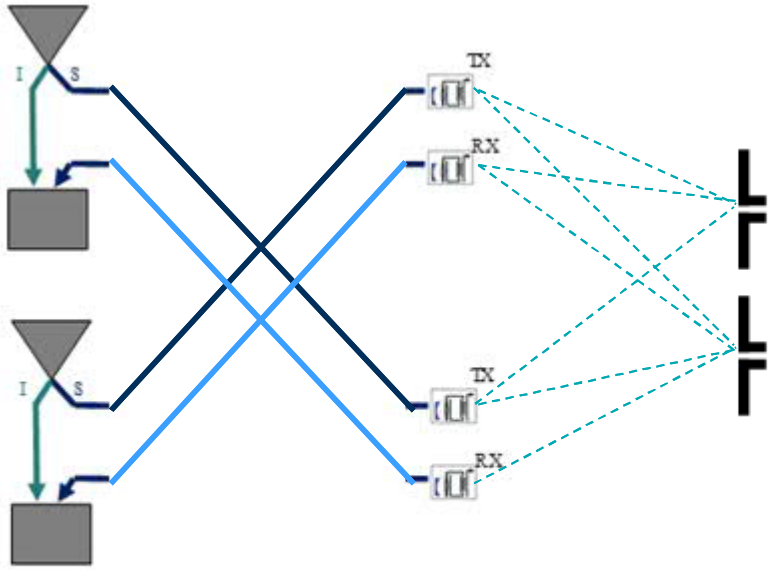

E-MIMO

Quantum MIMO channel

Beam-splitter model for a MIMO channel

$$\underbrace{\begin{bmatrix}\hat{a}_{R_1}\\ \hat{a}_{R_1}\end{bmatrix}}_{\mathbf{a}_R} = \underbrace{\begin{bmatrix}h_{11} & h_{12}\\ h_{21} & -h_{22}\end{bmatrix}}_{\mathbf{H}} \underbrace{\begin{bmatrix}\hat{a}_{S_1}\\ \hat{a}_{S_2}\end{bmatrix}}_{\mathbf{a}_S} + \underbrace{\begin{bmatrix}\hat{a}_{Z_1}\\ \hat{a}_{Z_2}\end{bmatrix}}_{\mathbf{a}_Z}$$

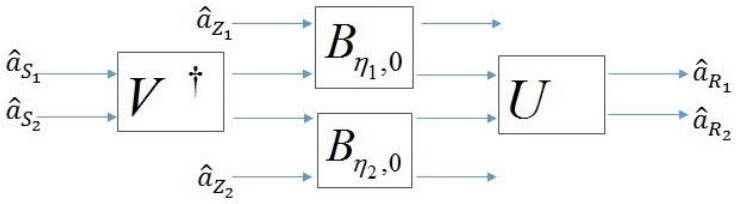

2x2 MIMO channel

Singular value decomposition

$$\mathbf{a}_R = \mathbf{U}\boldsymbol{\Sigma}\mathbf{V}^{\dagger}\mathbf{a}_S + \underbrace{\mathbf{U}\mathbf{S}\mathbf{a}_{Z'}}_{\mathbf{a}_Z}$$

$$\boldsymbol{\Sigma} = \begin{bmatrix}\sqrt{\eta_1} & \\ & \sqrt{\eta_2}\end{bmatrix}, \quad \mathbf{S} = \begin{bmatrix}\sqrt{1-\eta_1} & \\ & \sqrt{1-\eta_2}\end{bmatrix}$$

Quantum MIMO channel

N_t x r x N_r case

$$\text{rank}(\mathbf{H}) = r$$

$$\mathbf{a}_R = \mathbf{U}\boldsymbol{\Sigma}\mathbf{V}^{\dagger}\mathbf{a}_S + \underbrace{\mathbf{U}\mathbf{S}\mathbf{a}_{Z'}}_{\mathbf{a}_Z}$$

$$\boldsymbol{\Sigma} = \begin{bmatrix} \boldsymbol{\Sigma}_r & \\ & \mathbf{0}_{N-r} \end{bmatrix}, \quad \mathbf{S} = \begin{bmatrix} \mathbf{S}_r & \\ & \mathbf{0}_{N-r} \end{bmatrix}$$

Receive beam-former and transmitter pre-coding beam-splitters can be utilized to diagonalize the channel

$$\mathbf{U}^{\dagger}\mathbf{a}_R = \mathbf{U}^{\dagger}\mathbf{U}\boldsymbol{\Sigma}\mathbf{V}^{\dagger}\left(\mathbf{V}\mathbf{a}_S\right) + \mathbf{U}^{\dagger}\mathbf{U}\mathbf{S}\mathbf{a}_{Z'}$$
$$= \boldsymbol{\Sigma}\mathbf{a}_S + \mathbf{S}\mathbf{a}_{Z'}$$

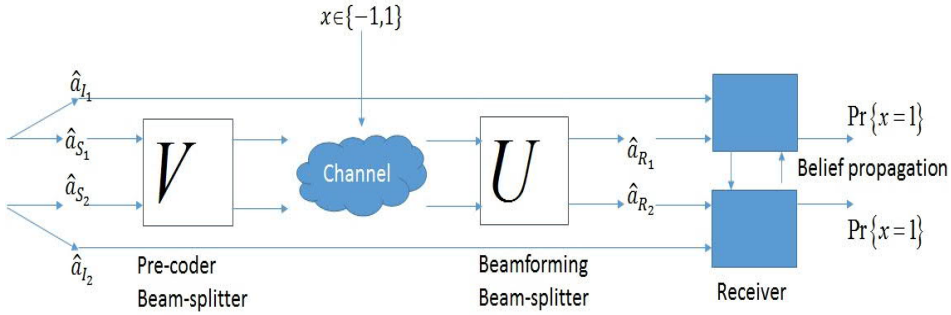

Beam-splitter decomposition

More than two antennas: Unitary operator can be built using beam-splitters

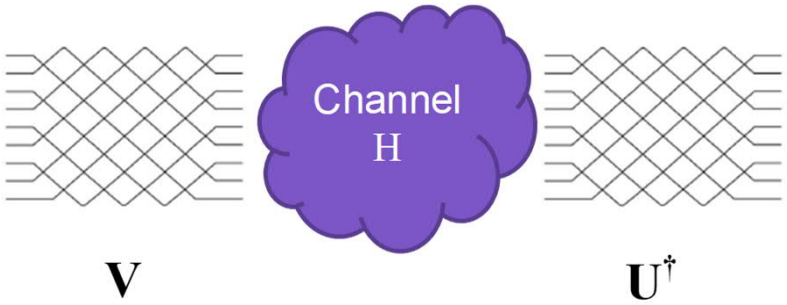

Clements, W.R., Humphreys, P.C., Metcalf, B.J., Kolthammer, W.S. and Walmsley, I.A., 2016. Optimal design for universal multiport interferometers. *Optica*, *3*(12), pp.1460-1465.

Beam-splitter pre-coding and receiver beam-forming

- The receiver can combine the results from the different radio paths using maximum ratio combining.
- Equivalent number of mode pairs

Parallel channels (P-MIMO):

$$\frac{M_P}{M} = \frac{N_r \frac{r}{N_r}}{\left(N_t - 1\right)\frac{r}{N_t}\beta + 1} \approx r$$

$$\beta \sim \frac{\eta N_S}{N_Z} << 1 \qquad \mathrm{tr}\left\{\mathbf{H}\mathbf{H}^{\dagger}\right\} = rN_r\eta$$

Eigen channels (E-MIMO):

$$\frac{M_E}{M} = rN_r$$

r is the rank of the channel probability amplitude matrix **H**

MIMO Backscatter Communications

Channel rank

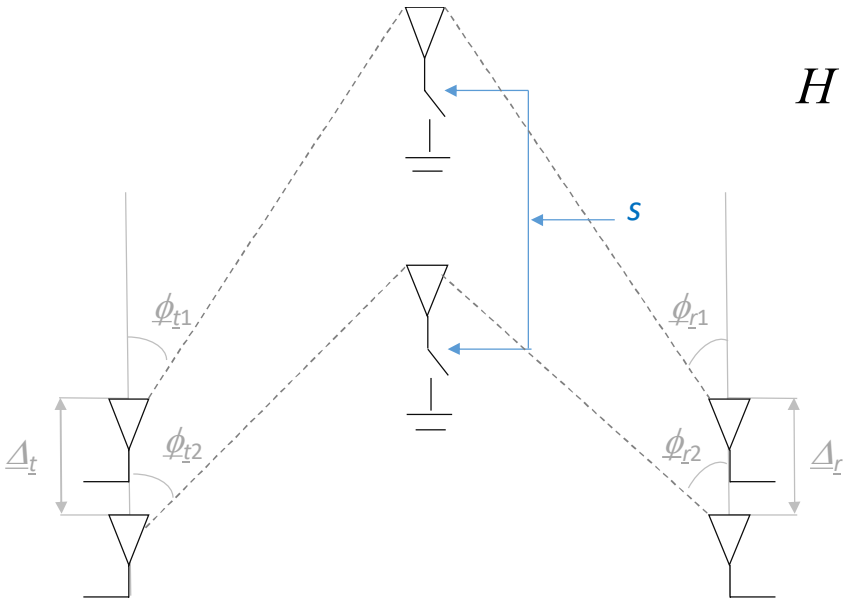

$$H = \sum_k \sqrt{\eta_k} e^{i\theta_k} \sqrt{n_t n_r} e_r\left(\Omega_{r,k}\right) e_t^{\dagger}\left(\Omega_{t,k}\right)$$

$$\text{rank}(H) = 2$$

$$\Omega_{t1} \neq \Omega_{t2} \bmod \frac{1}{\Delta_t}$$

$$\Omega_{r1} \neq \Omega_{r2} \bmod \frac{1}{\Delta_r}$$

MIMO Backscatter Communications

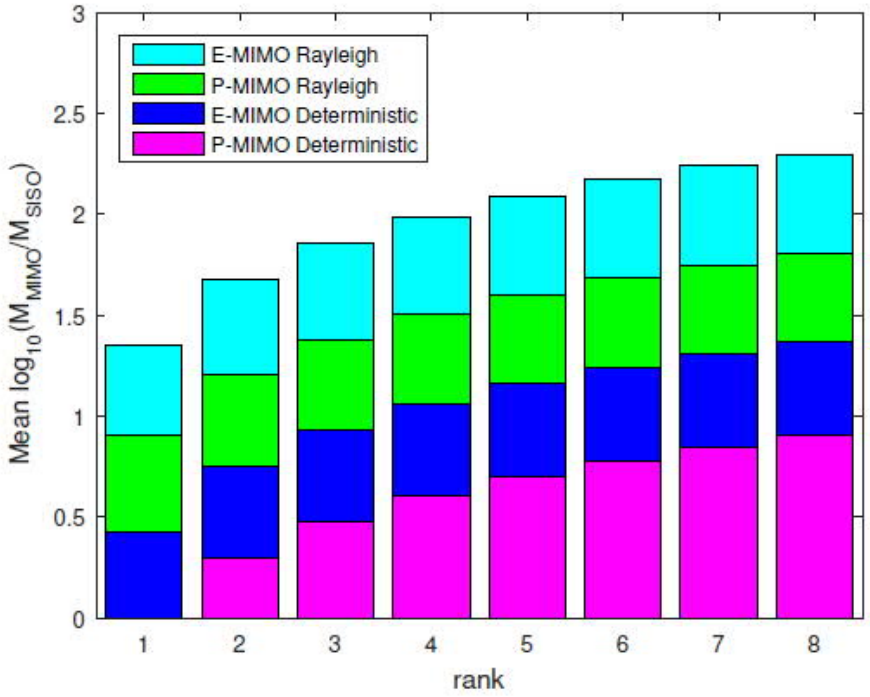

8x8 MIMO

R. Jäntti, R. Di Candia, R. Duan and K. Ruttik, "Multiantenna Quantum Backscatter Communications," *2017 IEEE Globecom Workshops (GC Wkshps)*, Singapore, 2017, pp. 1-6.

Practical implementation?

Is this a science fiction story?

Practical implementation?

No it's not. The required components exists.

- Superconducting microwave circuits
  - Phase shifters, beam-splitters,...
- Single microwave photon sources
- Single microwave photon detectors

Microwave Single Photon Source

- An artificial two-level system made of superconducting materials (Josephson Junctions) when excited by a microwave transmission line, will spontaneously emit a single photon.
- Efficiency is above 75% over a wide frequency range 6.7 to 9.1 GHZ

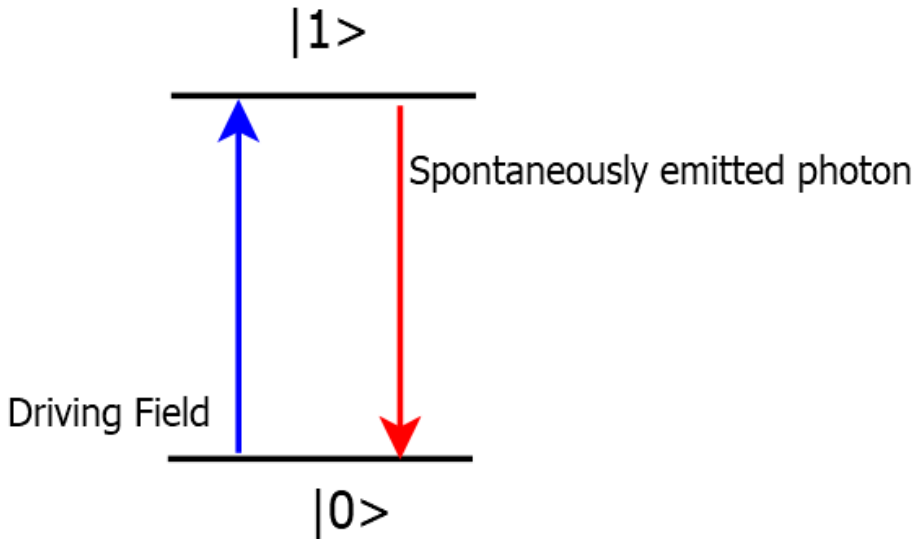

Z.H.Peng, et al.
"Tunable on-demand single-photon source in the microwave range",
Nature Communications **volume7**, 2016.

Two mode squeezed state generation

Fedorov, Kirill G., et al. "Displacement of propagating squeezed microwave states." *Physical review letters* 117.2 (2016): 020502.

Fedorov, K.G., Pogorzalek, S., Las Heras, U., Sanz, M., Yard, P., Eder, P., Fischer, M., Goetz, J., Xie, E., Inomata, K. and Nakamura, Y., 2018. Finite-time quantum entanglement in propagating squeezed microwaves. *Scientific reports*, *8*(1), p.6416.

Microwave Single photon detector

- Three level atomic configuration: an incoming photon drive the the transition between the |0> and |1> states, while a microwave transmission line drive that between |g> and |1>.
- Then the excited qubit will spontaneously emit a photon in the |1>→|g> mode. This is known as Raman transition. After that a click is registered to signal the detection of the incoming photon.
- single-photon-detection efficiency of 0.66 ± 0.06 with a low dark-count probability of 0.014 ± 0.001

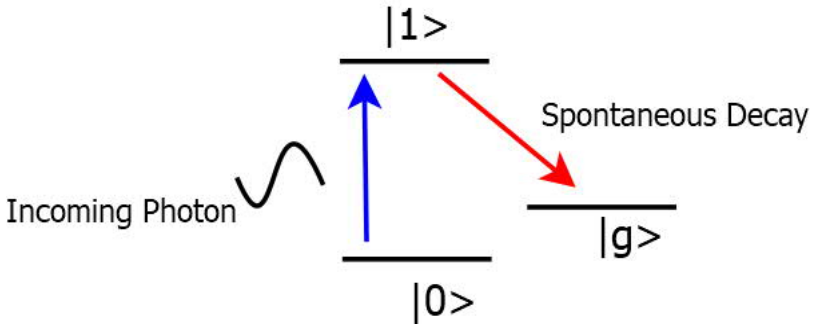

Kunihiro Inomata, et al.,"Single microwave-photon detector using an artificial Λ-type three-level system," *Nature Communications* **volume7**,2016

Quantum microwave link

- Xian e.t. al have proposed a general protocol for sending quantum states through thermal channels, even when the number of thermal photons in the channel is much larger than 1.
- The protocol can be implemented with state-of-the-art superconducting circuits and enables the transfer of quantum states over distances of about 100 m via microwave transmission lines cooled to only T=4 K.

Xiang, Z.L., Zhang, M., Jiang, L. and Rabl, P., 2017. Intracity quantum communication via thermal microwave networks. *Physical Review X*, *7*(1), p.011035.

Quantum FM receiver

- Researchers at Delft University of Technology have created a quantum circuit that enables interfacing quantum circuits operating in mK temperatures with megahertz systems in ambient temperature.

Mario F. Gely, Marios Kounalakis, Christian Dickel, Jacob Dalle, Rémy Vatré, Brian Baker, Mark D. Jenkins, Gary A. Steele, *Observation and stabilization of photonic Fock states in a hot radio-frequency resonator*, Science, 7 March 2019

Conclusions

- Quantum illumination can be utilized to enhance the performance of backscatter communications
- Up to 6 dB bit error exponent gain is possible for OOK and BPSK and up to 3 dB gain for QPSK
- One of the limiting factor of the QI-based inference on the microwave domain is the low rate at which the entangled photon pairs can be generated.
- Multiple antennas can be utilized to generate so called virtual modes.
  - Eigenchannel MIMO can be realized using beam-splitters
- Multiple antennas are also needed to mitigate the impact of clutter.
- Equipment for performing experimentation is emerging

Back/re-scatter for IoT

- **New layer of backscatter commuinications could be added to underlay existing and emerging communication systems.**

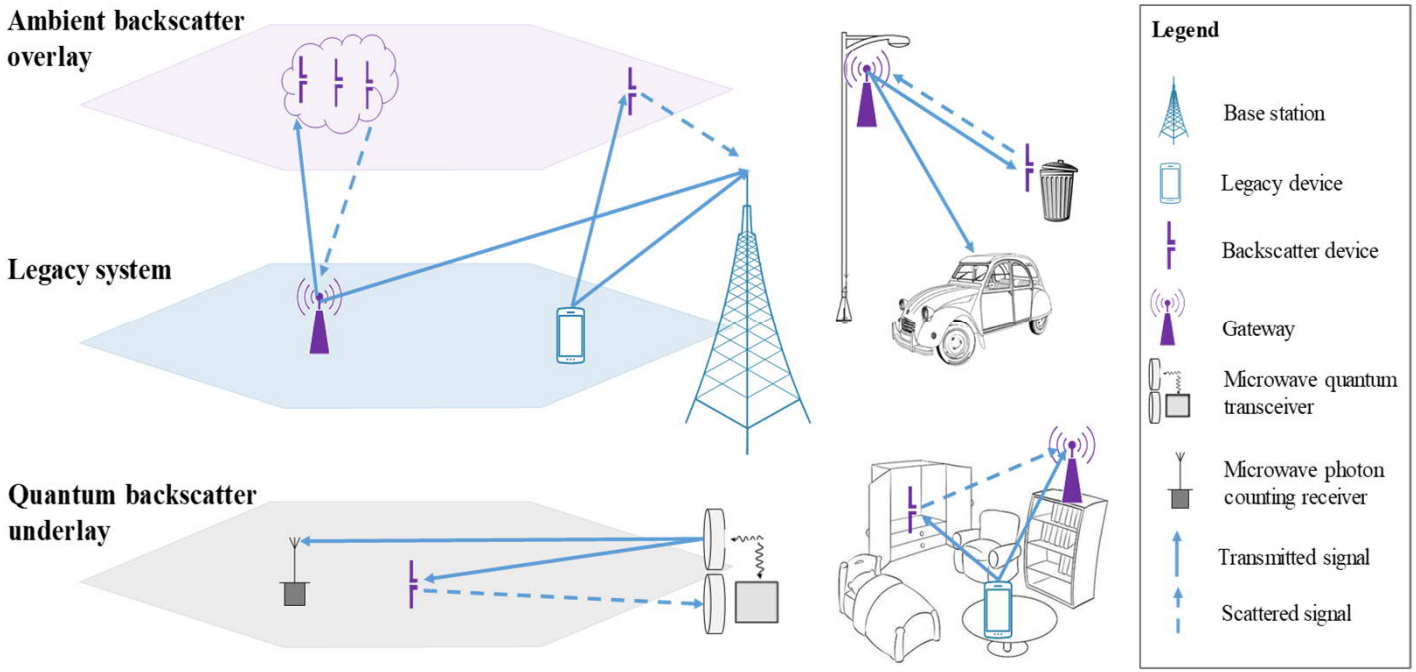

Aalto University
School of Electrical
Engineering

Department of Communications
and Networking (Comnet)